Hilbert-space structure of a solid-state quantum computer: Two-electron states of a double-quantum-dot artificial molecule

Xuedong Hu and S. Das Sarma

Department of Physics, University of Maryland, College Park, Maryland 20742-4111

We theoretically study a double-quantum-dot hydrogen molecule in the GaAs conduction band as the basic elementary gate for a quantum computer, with the electron spins in the dots serving as qubits. Such a two-dot system provides the necessary two-qubit entanglement required for quantum computation. We determine the excitation spectrum of two horizontally coupled quantum dots with two confined electrons, and study its dependence on an external magnetic field. In particular, we focus on the splitting of the lowest singlet and triplet states, the double occupation probability of the lowest states, and the relative energy scales of these states. We point out that at zero magnetic field it is difficult to have both a vanishing double occupation probability for a small error rate and a sizable exchange coupling for fast gating. On the other hand, finite magnetic fields may provide finite exchange coupling for quantum computer operations with small errors. We critically discuss the applicability of the envelope-function approach in the current scheme, and also the merits of various quantum-chemical approaches in dealing with few-electron problems in quantum dots, such as the Hartree-Fock self-consistent-field method, the molecular-orbital method, the Heisenberg model, and the Hubbard model. We also discuss a number of relevant issues in quantum dot quantum computing in the context of our calculations, such as the required design tolerance, spin decoherence, adiabatic transitions, magnetic-field control, and error correction.

PACS number(s): 03.67.Lx, 73.20.Dx, 85.30.Vw

I. BACKGROUND

In recent years there has been a great deal of (as well as a growing) interest throughout the physics community in quantum computation and quantum computers (QC's) [1], in which microscopic degrees of freedom such as atomic levels and electron spins play the role of quantum bits (qubits). Because of the inherent entanglement and superposition during the *unitary* evolution of multiple qubits, QC's can perform certain tasks such as factoring large integers [2], exponentially faster than classical computers. They also have significant advantages over classical computers in tasks such as searching [3] and simulating quantum mechanical systems [4,5]. Moreover, quantum error correction codes have been discovered [7], which further bolster the hope for a practical quantum computer. Various QC architectures have been proposed in the literature. The basic ingredients for a QC are two-level elements serving as qubits, controlled single- and two-qubit unitary operations, exponentially large and precisely defined (i.e., no mixing with other states) Hilbert space, weak decoherence, and single qubit measurements [6]. One of the earliest QC proposals uses electronic energy levels of ions in a linear trap (an ''ion trap'' QC) as qubits [8,9]. Optical pulses perform single-qubit operations, while two-qubit operations are provided by multiple optical pulses with the lowest vibrational mode of the ion chain as an intermediary. In another proposed QC architecture, the cavity QED QC [10,11], photon polarization provides the two required states for a qubit. The polarization state can be rotated optically, which provides single-qubit operations. Two-qubit operations are achieved with the intermediary of a trapped atom in the cavity using the atom-photon interaction. Yet another proposed QC architecture uses bulk NMR techniques, where the individual nuclear spins in a molecule are the qubits, with different locations on the molecule as tags for each qubit. Radio-frequency electromagnetic pulses provide single-qubit operations, while dipolar interaction between nuclear spins is used for two-qubit operations. Final-state detection in the NMR QC is achieved through an ensemble average over all the molecules in the entire bulk solution. Single- and two-qubit operations have so far been demonstrated in trapped ions [9], photons in a microcavity [11], and nuclear spins in bulk solutions [12]. One perceived shortcoming of all these approaches, however, is their lack of scalability. For example, it has been pointed out that the NMR approach (which is considered to be a promising QC architecture) cannot go beyond 20 qubits because of an exponentially diminishing signal-to-noise ratio as the number of qubits increases [12]. For the ion trap and cavity QED QC systems it is hard to see how one would surpass only a few qubits. Thus the atomic-molecular systems, which have so far demonstrated single- and perhaps even two-qubit operations, are unlikely to lead to an operational QC due to severe scalability problems.

There have been several recent proposals for solid-state quantum computers, with superconducting Cooper pairs [13], electron spins [14,15], electron orbital energy levels in nanostructures [16], and donor nuclear spins [17] serving as qubits. A solid-state quantum computer, if it can ever be built, holds a decisive advantage in scalability compared to the atomic-molecular systems mentioned above. However, strong decoherence, the intrinsic difficulty in obtaining precise microscopic control, and inherently complicated Hilbert space are key roadblocks on the way to a practical solid-state QC. In fact, no demonstration of even a single-qubit operation has yet been achieved in a solid-state QC, and thus the subject of developing reasonable QC hardwares faces an un-

enviable dichotomy: QC systems with demonstrated qubits are difficult to scale up, while proposed scalable QC systems do not have any qubits.

In this paper we study a solid-state QC architecture which uses electron spins in two-dimensional horizontally coupled quantum dots as qubits [14]. Here a single electron is trapped in each individual quantum dot. Spins of these trapped electrons are qubits, while the quantum dots in which they reside provide tags for each qubit. Single-qubit operations, involving the modification of local electronic spin states in each dot, are to be performed using external local-magnetic-field pulses, while two-qubit operations are realized using the exchange interaction between two electrons in neighboring quantum dots. Since electron-spin eigenstates usually have very long coherence times compared with electron orbital states [18,19], spin states may be better candidates for the role of qubits. Although a microscopically local magnetic field is not a standard feature of modern condensed-matter experiments, reasonable proposals for the local manipulation of spin states have been put forward [14]. Exchange interaction can be tuned by various means, including external gate potentials and external magnetic fields. An important point is that a single electron spin can, in principle, be detected by superconducting quantum interference device magnetometers, and it has been proposed that single-electron-spin detection can also be done by transferring the spin information to charge degrees of freedom, which can then be detected via the sensitive single-electron transistor technique [20]. The spin-based quantum-dot quantum computer proposal clearly has important merits and deserves serious consideration. Much theoretical work, however, is needed to investigate whether the design tolerance required for QC operations can actually be achieved in the state of the art quantum-dot systems. In this study we focus on the Hilbert space structure of coupled quantum-dot systems, and its implications for quantum computing. One of our specific goals is to ascertain, through fairly extensive numerical computations, whether the spin-based quantum-dot QC is a feasible proposal even from an idealized theoretical perspective. We believe that such a theoretical study is necessary before one could seriously consider the fabrication of a quantum-dot QC.

II. INTRODUCTION

There are many different ways to fabricate a quantum dot [21]. In GaAs, which is the system we nominally consider in this paper, one common approach is to apply external electric fields through lithographically patterned gates to produce a depletion area in a two-dimensional electron gas. In particular, nanoscale electrodes are created on the surface of a heterostructure using photolithography. The application of appropriate electric voltages over the electrodes then produces a suitable confining potential, thus creating areas where electrons have been pushed away at desired locations (depletion areas). The typical size of this type of dot, with currently available lithographic techniques, is generally large (in the order of 100×100 to 1000×1000 nm^2). The important physical parameters for such a quantum dot are the shape and strength of the confinement potential, the number

of electrons trapped, the strength of the electron-electron interaction, the strength of the additional external fields (magnetic, electric, etc.), impurities, surface roughness, boundary irregularities, etc. Substantially smaller size quantum dots can be made by direct material growth techniques, such as quantum-dot self-assembly, but it has been difficult to add electrons to such self-assembled dots, making QC architecture difficult.

The study of semiconductor quantum dots and other nanostructures has been a large and fast developing field in the past ten years [22]. There are, however, relatively few works concentrating on the properties of two electrons in a coupled double-dot system, or an artificial hydrogenic quantum-dot molecule, which is the subject of our work. Among related studies, quantum-dot He (two electrons in a single quantum dot) has been theoretically investigated [23,24]. A vertically coupled double-quantum-dot system has also been theoretically [25–29] and experimentally [30–33] studied. The horizontally coupled double-dot ''hydrogen'' molecule, which is the focus of the current paper, has been studied experimentally and theoretically in the context of transport and optical (or infrared) spectroscopic experiments [34–38], and very recently the case when there are only two electrons in the double-dot structure has been treated theoretically [39] in a rather simple approximation scheme using the Heitler-London and Hund-Mulliken molecular-orbital approaches. An additional complication in the case of horizontally coupled dots is that the z-direction angular momentum is not conserved because of the absence of the cylindrical symmetry, while this symmetry can be used to simplify calculations in the case of a single quantum dot or a vertically coupled dot. This lack of z angular momentum conservation makes our calculation substantially more complicated than earlier quantum-dot electronic structure calculations [23–28] in single-dot and vertically coupled-dot structures.

In this paper we present our study of the Hilbert space structure of a horizontally coupled double-quantum-dot system, as shown schematically in Fig. 1. Such a horizontally coupled double-quantum-dot system, with suitable lithographic gates to control the interdot coupling, is one of the minimal requirements for a spin-based quantum dot QC. Vertically coupled double dots might not be as good a candidate for the purpose of quantum computing because the coupling between the dots cannot be tuned as easily, while the tuning of interdot coupling is essential in the two-qubit operations. QC operation requires a very special Hilbert-space structure with a very large and a precisely defined state space. In the electron-spin-as-qubit proposal we consider in this paper, one crucial condition is the isolation of the electron spins from their environment, including the electronic orbital degrees of freedom. For example, if a doubly occupied state (with two electrons in the same orbital state of a single quantum dot) is easily accessed, when the two electrons separate again, one loses all the information about the identification of the spins (the ''tags''). Therefore, one stringent requirement is that the Hilbert space should be such as not to allow appreciable double occupation. This is, however, quite tricky, since the double occupation probability obviously depends on interdot tunneling which cannot be
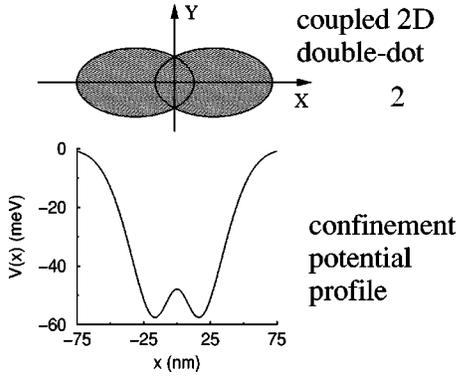
FIG. 1. This is the schematics of the double-dot system we studied. We use Gaussian potential wells and a Gaussian central barrier. Unless otherwise specified, the dot size is 30 nm in radius. When the two dots are separated by 30 nm, we study three cases where the central potential barrier has strengths V_b of 20, 25, and 30 meV, corresponding to effective barrier heights of 3.38, 6.28, and 9.61 meV, respectively. When the two dots are separated by 40 nm, we show results of three cases where V_b takes values of 13.86, 18.17, and 20 meV, corresponding to actual barrier heights of 6.28, 9.61, and 11.03 meV.

zero if there is to be an appreciable exchange coupling (which is required for two-qubit operations in the current model). The goal of the current study is to obtain the Hilbert space for a two-electron double-dot system using reasonably realistic quantum-chemical techniques. Since single- and two-qubit operations are the only operations necessary for quantum computing [1], our study would be exploring the envelope of the needed Hilbert space (for QC) and its proximity to the unwanted excited-state space. We are to assess the constraints and tolerance required to fabricate a spin-based quantum-dot QC system. We will go beyond the simple Heitler-London and Hund-Mulliken models and take into consideration electron correlation through a larger basis in the molecular-orbital calculation. We use several approximations of varying complexity in our electronic structure calculations in order to obtain a realistic estimate of the theoretical computational work which will be needed to provide the underlying basis for fabricating a spin-based quantum-dot QC.

III. THEORY

A. Model Hamiltonian

In the current study we use a single-conduction-band effective-mass envelope function to describe the confined electrons in two-dimensional (2D) GaAs quantum dots. Such an approach is valid if the characteristic energy corresponding to the envelope function is much smaller than the fundamental band gap. In addition, the excitation energy along the third (growth) direction has to be much larger than all the characteristic 2D excitation energies. In the case of GaAs, the fundamental gap is 1.5 eV. Furthermore, for a 10-nm-thick 2D GaAs quantum well (which hosts the quantum dot), the first intersubband excitation energy (for excitations along the growth direction) is typically 0.1 eV. Since the charac-

teristic in-plane 2D excitation energy of the confined electron(s) is on the order of 1–10 meV, the applicability criterion for the effective-mass single-envelope-function approximation is well satisfied. The effective two-electron quantum dot molecule Hamiltonian in the presence of an external magnetic field (defined through the vector potential **A**) is then

$$H = \sum_{i=1}^{2} \left[\frac{1}{2m^*} \left(\mathbf{p} + \frac{e}{c} \mathbf{A}(\mathbf{r}_i) \right)^2 + V(\mathbf{r}_i) + g^* \mu_B \mathbf{B} \cdot \mathbf{S}_i \right] + \frac{e^2}{\epsilon r_{12}},$$
(1)

where m^* is the conduction-electron effective mass, $V(\mathbf{r}_i)$ is the quantum-dot potential (which is to be parametrized in our work, but can in principle be calculated by self-consistent techniques if the details of the electrostatic confinement are known), g^* is the effective electron g factor, μ_B is the Bohr magneton, $g^* \mu_B \mathbf{B} \cdot \mathbf{S}_i$ is the Zeeman splitting, ϵ is the static background (lattice) dielectric constant, and r_{12} is the distance between the two electrons. Here we uncritically assume the effective-mass approximation (which we will show to be well valid), assuming the interband mixing to be negligibly small in the low-energy sector of our interest and the effect of the periodic crystal potential to be described by the electron effective mass and the background dielectric constant. The quantum-well material we focus on in this work is GaAs; thus $g^* \approx -0.44$, $\epsilon \approx 13.1$, and $m^* \approx 0.067m_0$, where m_0 is the bare electron mass. As our model 2D quantum-dot confinement potential we use the following linear combination of three Gaussians defined by the adjustable parameters V_0, a, V_b, l_x, l_y, l_{bx}, and l_{by}:

$$V(\mathbf{r}) = V_0 \left[\exp\left(-\frac{(x-a)^2}{l_x^2} \right) + \exp\left(-\frac{(x+a)^2}{l_x^2} \right) \right]$$
$$\times \exp\left(-\frac{y^2}{l_y^2} \right) + V_b \exp\left(-\frac{x^2}{l_{bx}^2} \right) \exp\left(-\frac{y^2}{l_{by}^2} \right). \quad (2)$$

Here the first two Gaussians (with a strength of V_0) are for the individual dot potential wells, and the third (with a strength of V_b) is for controlling the central barrier (so that we can adjust the barrier easily and independent of the locations of the other two Gaussians). Thus V_0 is the potential well depth, while V_b controls the central potential barrier height. We choose this form for the confinement potential mainly because of its simplicity and versatility, and no other particular significance should be attached to our choice. To find a realistic form for V requires a self-consistent calculation using the correct boundary conditions and heterostructure parameters, which is not warranted at the current level of QC modeling (and is well beyond the scope of this work). We only note here that the confinement potential defined by Eq. (2) is a reasonable potential for 2D double-quantum-dot structures defined electrostatically, provided the confinement along the growth (z) direction is much tighter than the 2D confinement as discussed above. It is easy to fit a realistic confinement potential, if available, to this simple Gaussian form.

The two-electron Hamiltonian cannot be solved exactly. We use two different approaches to calculate the approximate energy spectra and electron states of the Hamiltonian H defined by Eq. (1). The first is a Hartree-Fock (HF) calculation, where the two electrons are treated as independent particles moving in a HF self-consistent field [40]. The second is the so-called molecular-orbital method, in which we use single-harmonic-well single-electron wave functions to form two-electron orbitals, and use them as basis states to solve the Schrödinger equation for the two electrons [40]. We note that the presence of the external magnetic field makes our problem somewhat different from the standard quantum-chemistry calculations.

B. Hartree-Fock approximation

In the HF approximation, an electron is moving in the mean field produced by all other electrons. The multiple-electron wave function is a single Slater determinant. The Pauli principle is thus obeyed, so that electrons with the same spin do not occupy the same orbital state simultaneously. Electron correlation is therefore taken into account crudely in the sense that only the Pauli-principle-imposed correlations are included. There are a variety of Hartree-Fock calculations in the context of quantum chemistry [40]. In our study here, a restricted Hartree-Fock (RHF) calculation, where the two electrons with different spins occupy the same spatial orbital, significantly overestimates the double occupation probability and thus overestimates the energy of a singlet state. Such a RHF calculation is clearly a rather poor approximation for our purpose, where an accurate knowledge of the double occupation probability and of the singlet-triplet splitting is an important requirement. Therefore, we adapt an unrestricted Hartree-Fock (UHF) approach [38], where the two electrons in the ground state with opposite spins are not required to occupy the same spatial orbital. This method inherently incorporates the uncorrelated nature of two remote quantum dots, which is partially satisfactory for our purpose. However, a shortcoming of this approach is that the ground state (where the spins of the two electrons are opposite) is not a pure singlet state.

The HF equations for N electrons are

$$F\psi_i(\mathbf{r}_1) = E_i\psi_i(\mathbf{r}_1),$$

$$F = f + \sum_{j=1}^{N} (J_j - K_j),$$

$$f = \frac{1}{2m^*}\left[\mathbf{p} + \frac{e}{c}\mathbf{A}(\mathbf{r}_1)\right]^2 + V(\mathbf{r}_1), \qquad (3)$$

$$J_j\psi_i(\mathbf{r}_1) = \int \psi_j^*(\mathbf{r}_2)\psi_j(\mathbf{r}_2)\frac{e^2}{\epsilon r_{12}}d\mathbf{r}_2 \cdot \psi_i(\mathbf{r}_1),$$

$$K_j\psi_i(\mathbf{r}_1) = \int \psi_j^*(\mathbf{r}_2)\psi_i(\mathbf{r}_2)\frac{e^2}{\epsilon r_{12}}d\mathbf{r}_2 \cdot \psi_j(\mathbf{r}_1).$$

Here ψ_i ($i=1,\ldots,N$) are the appropriate single-particle wave functions; f is the single-particle part of the Fock operator F, which has the same form as the corresponding terms of Eq. (1); the operator J_i is the direct Coulomb repulsion between two electrons; and the operator K_i is the exchange interaction between electrons. All the integrals include sums over different spin indices. In other words, the exchange term K_j vanishes if the spin indices of the jth and ith electron orbitals are different.

The advantage of HF approximation lies in its clear physical picture of an effective single-particle dynamics in a self-consistent-field background. However, its shortcoming is also due to this simplicity: electrons only ''see'' an average background produced by the other charges, not the instantaneous locations of those charges, and therefore electron correlation is not taken into account beyond the Pauli principle (which is built into the Slater determinant). In addition, in numerically solving the HF equations in the presence of a finite magnetic field, the choice of gauge turns out to be important, a fact which we have not found to have been discussed earlier in the literature. When the two electrons are well separated and each is confined to its own well, they should have their own gauges; if the electron wave functions are extended throughout the two wells, then a single gauge has to be used. The use of a single gauge, however, significantly raises the Coulomb repulsion energy of the electrons, because the $\mathbf{A}^2$ term can be quite large in high magnetic fields, thus behaving like an additional confining harmonic potential, pushing the two electrons toward each other. It is interesting to reflect on why gauge invariance breaks down in this HF calculation. It certainly should hold for the exact two-electron Schrödinger equation, in contrast to the HF approximation. However, as we make Hartree-Fock approximations, we mostly neglect the electron-electron correlations. The choice of gauge thus becomes relevant to our approximate calculation. This point is further illustrated by the fact that the exact two-electron wave function is a superposition of an infinite number of Slater determinants. As these determinants generally transform in different ways under a gauge transformation, the change in the overall wave function can be quite different from that of each individual Slater determinant. The breakdown of the gauge invariance in the HF approximation thus arises from its very special single Slater determinant form. The broken gauge invariance shows a glaring weakness of the Hartree-Fock approach which clearly needs to be supplemented by other techniques in order to obtain a more complete description of the two-electron system. Below we discuss another quantum-chemical approach that can better describe the electron correlations.

C. Molecular-orbital method

For a two-electron problem, the molecular-orbital approach involves choosing suitable single-electron basis functions, forming two-electron orbitals from these basis functions, expanding the two-electron Schrödinger equation in these two-electron orbitals, and finally solving the eigenvalue problem (presumably through a direct matrix diagonal-

ization). In our molecular-orbital calculation, we use single-dot single-electron wave functions as the basis states to form our molecular orbitals. These single-electron wave functions are the usual Fock-Darwin states (assuming parabolic confinement at the bottom of the potential wells) [21]. We take care in ensuring that our two-electron wave functions have the correct symmetry of our two-particle Hamiltonian defined in Eq. (1). In the simplest case (the so-called Hund-Mulliken approximation), we use only the two single-dot ground eigenstates (s orbitals) as the basis states. These wave functions take the following form for a symmetric quantum-dot structure with identical confinement along x and y directions [21,39]:

$$\phi_{\mp a,\ or\ L/R}(x,y)=\frac{1}{\sqrt{\pi}l_0}\exp\left[\frac{(x\pm a)^2+y^2}{2l_0^2}\right]\exp\left(\mp i\frac{ay}{2l_B^2}\right),$$

(4)

where

$$l_0=\frac{l_B}{\sqrt[4]{1/4+\omega_0^2/\omega_c^2}},$$

$$l_B=\sqrt{\frac{\hbar c}{eB}},$$

(5)

$$\omega_c=\frac{eB}{m^*c}.$$

Here $\pm a$ are the potential minima locations of the two quantum dots which are horizontally placed along the x direction; l_0 is the effective wave-function radius; l_B is the magnetic length for the applied magnetic field B along the z direction; ω_0 is the confinement parabolic well frequency; ω_c is the electron cyclotron frequency; and m^* is the GaAs conduction-electron effective mass. The gauge that produces the above wave function is $\mathbf{A}=(B/2)(-y,x,0)$. Note that in choosing our single-particle basis to form the molecular orbitals we use the exact one-electron eigenstates corresponding to a double parabolic well 2D potential which is obtained by expanding the Gaussian potential well of Eq. (2) around its minima. This particular basis has the great advantage of being analytic (the Fock-Darwin levels) as well as a reasonable basis for the problem we are to solve. Using the single-dot wave functions $\phi_{L/R}(\mathbf{r})$, the corresponding triplet wave function is $\Psi_1=[\phi_L(\mathbf{r}_1)\phi_R(\mathbf{r}_2)-\phi_L(\mathbf{r}_2)\phi_R(\mathbf{r}_1)]/\sqrt{2}$, while the singlet wave functions are $\Psi_2=[\phi_L(\mathbf{r}_1)\phi_R(\mathbf{r}_2)+\phi_L(\mathbf{r}_2)\phi_R(\mathbf{r}_1)]/\sqrt{2}$, $\Psi_3=\phi_L(\mathbf{r}_1)\phi_L(\mathbf{r}_2)$, and $\Psi_4=\phi_R(\mathbf{r}_1)\phi_R(\mathbf{r}_2)$. It is clear that this basis consists of the Heitler-London states Ψ_1 and Ψ_2 and the two ''ionized'' or ''polarized'' doubly occupied states Ψ_3 and Ψ_4. We can solve the Schrödinger equation for the two-electron Hamiltonian in this basis by expanding in these four functions. Since the triplet state is antisymmetric in the orbital degrees of freedom while singlet states are symmetric, they are not coupled by the symmetric Hamiltonian of Eq. (1). Thus triplet and singlet states can be treated separately. Note that the

two-electron states are generally neither orthogonal nor normalized because the single-dot single-electron wave functions $\phi_L(\mathbf{r})$ and $\phi_R(\mathbf{r})$ are not orthogonal to each other. Thus the Schrödinger equation of the problem can be expressed as

$$\sum_j^4 H_{ij}c_j=E_i\sum_j^4 S_{ij}c_j,$$

$$H_{ij}=\int \Psi_i^*(1,2)H\Psi_j(1,2)d\mathbf{r}_1d\mathbf{r}_2,$$

(6)

$$S_{ij}=\int \Psi_i^*(1,2)\Psi_j(1,2)d\mathbf{r}_1d\mathbf{r}_2.$$

We now have a generalized eigenvalue problem. It can be readily solved numerically. Formally, it is identical to an ordinary eigenvalue problem if we know the inverse of S.

To systematically improve upon the four-state molecular orbital calculation, we include the first excited states of single quantum dots (p orbitals) in an improved (so-called s-p hybridized) molecular-orbital calculation. The single-particle p orbitals have the following forms:

$$\phi_{1,\pm 1,-a}(x,y)=\frac{1}{\sqrt{\pi}l_0^2}[(x+a)\pm iy]\exp\left[\frac{(x+a)^2+y^2}{2l_0^2}\right]$$

$$\times\exp\left(-i\frac{ay}{2l_B^2}\right),$$

(7)

$$\phi_{1,\pm 1,a}(x,y)=\frac{1}{\sqrt{\pi}l_0^2}[(x-a)\pm iy]\exp\left[\frac{(x-a)^2+y^2}{2l_0^2}\right]$$

$$\times\exp\left(i\frac{ay}{2l_B^2}\right).$$

Here the first two subindices are the quantum numbers for the Fock-Darwin states, while the third one indicates their locations. Now we have six (two s orbitals and four p orbitals) atomic orbitals (single-electron single-dot eigenstates), with which we can form 21 singlet states and 15 triplet states. Since parity symmetry is not broken by the introduction of a magnetic field, we can introduce even and odd single-electron molecular orbitals, and then build the two-electron molecular orbitals using these symmetrized orbitals. There are then 12 even singlet states, nine odd singlet and triplet states, and six even triplet states. The use of parity reduces the number of independent two-particle matrix elements almost by half. The advantage of introducing the p orbitals in the molecular-orbital calculation is that the excited states give us the freedom to form anisotropic states (which could not be accomplished with the isotropic s-orbital-only basis), thus enabling us to describe electron overlap with higher accuracy.

IV. NUMERICAL RESULTS

A. Hartree-Fock approximation

In our HF calculation, we solve numerically the Hartree-Fock equations by setting up a grid of 60×30 mesh points on the two-dimensional (x,y) space. The reason for not se-
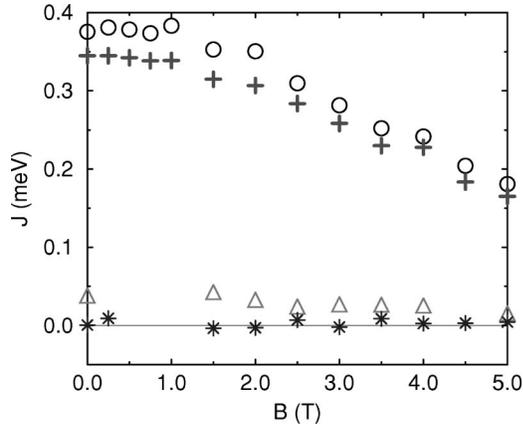
FIG. 2. Here we show the magnetic-field (B) dependence of the energy splitting (J) between parallel and opposite spin states calculated by the unrestricted Hartree-Fock approach. The two higher-energy curves are for dots with 30-nm radius, 30-nm interdot separation, and 20-meV V_b. The lower-energy ones are for dots with 70-nm radius and 80-nm dot separation. Between the two higher-energy sets of data, the slightly lower one has a slightly thicker (l_{bx} larger by 2 nm) central barrier. The two sets of data for larger dots differ by central barrier heights (V_b) of 20 and 40 meV.

lecting a finer mesh for the grid is that we have a coupled two-dimensional problem that is not sparse, so that the actual nonsparse matrix dimension reaches 1800×1800, which is essentially our computation limit. We make a nonlinear transformation of the spatial coordinates so that most of the grid points are within the two-dot region, thus ensuring the accuracy and effectiveness of our numerical eigensolutions.

Figures 2 and 3 show some of the results we obtain using the UHF approximation. In Fig. 2 we can see that the energy of the lowest parallel spin (triplet) state remains above the lowest opposite spin state, and never dips below it up to a fairly high magnetic field of 7 T for reasonable quantum-dot
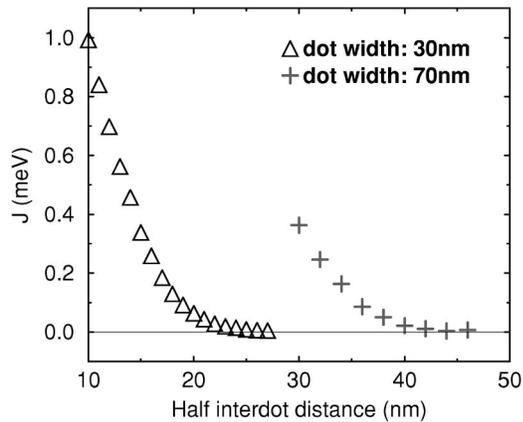

FIG. 3. Here we show the interdot distance dependence of the energy splitting (J) between parallel and opposite spin states calculated by the unrestricted Hartree-Fock approach. The left set of data corresponds to the small dot (30-nm radius and 20-meV V_b) case, and the right set of data to the large dot (70-nm radius and 20-meV V_b) case. A steep decrease in the energy splitting is present in both cases.

parameters as given in the figure captions. Notice that in the UHF theory the opposite spin state is actually a mixture of a singlet state and a triplet state, and therefore the ground state is never a pure singlet state. Although a RHF approach would have produced a pure singlet eigenstate, it significantly overestimates the Coulomb energy so that the singlet state always has higher energy than the triplet state, violating the theorem that at zero magnetic field (when the wave function can be written as a real function) the ground state should be a singlet [42]. In Fig. 3 we show two sets of data where the ground-triplet splitting decreases *exponentially* quickly as a function of the interdot distance. This suggests that, at least in principle, an efficient control of the splitting between the ground and first excited states can be achieved by increasing the potential barrier separating the dots and/or by increasing the interdot separation.

A simple Hartree-Fock calculation with a single Slater determinant is generally not sufficiently accurate to deal with subtle effects arising from small interaction terms in the Hamiltonian. For instance, since the reason for the singlet-triplet crossing is essentially two-electron exchange and correlation effects, the Hartree-Fock approximation should not be trusted to produce quantitatively reliable singlet-triplet splitting information (although it is expected to be qualitatively correct since exchange, which the HF theory includes, is expected to be the dominant effect). Our main reason for pursuing the HF theory, in spite of its obvious quantitative shortcoming, is the fact that the self-consistent HF calculation produces a more accurate single-particle wave function than the eigenstates of a fixed harmonic well. Based on these improved single-particle HF states, a configuration-interaction (CI) calculation can then be built in the future, which will lead to a more faithful and quantitatively accurate description of the actual two-electron wave functions in the double-quantum-dot system. Our HF calculation could be the starting point of such a future CI calculation.

B. Molecular-orbital methods

The central task in our molecular-orbital calculation is the computation of two-particle (Coulomb) matrix elements in the molecular orbital basis set described in Sec. III of this paper. In the Hund-Mulliken calculation (using only the s orbitals) which involves a basis of three singlet states (the Heitler-London Ψ_2 state and the two doubly occupied states Ψ_3 and Ψ_4) and one triplet state, we need to calculate only seven Coulomb matrix elements (taking even-odd-parity symmetry into consideration, only five Coulomb matrix elements are needed). When p orbitals are included, we need to calculate 231 and 120 Coulomb matrix elements for the singlet and triplet states, respectively, which is a substantial computational task. When the even-odd symmetry is taken into account, the number of Coulomb matrix elements reduces to 123 and 66, respectively, for the singlet and triplet states, which is still a formidable task because each matrix element corresponds to a four-dimensional integral requiring high accuracy. The most computationally intensive and time consuming part of our calculations has been the evaluation of these Coulomb matrix elements.
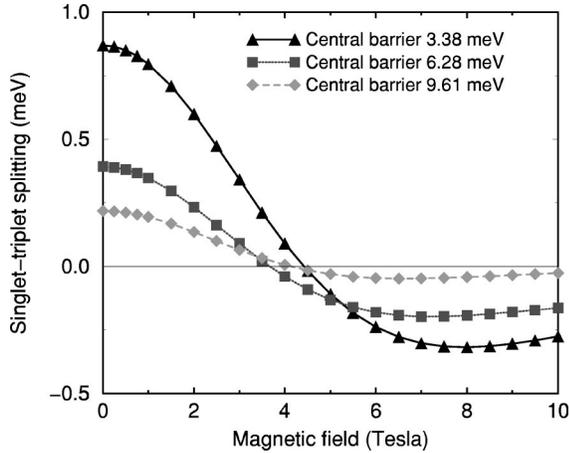
FIG. 4. Here we show the magnetic-field dependence of the singlet-triplet splitting in a Hund-Mulliken calculation for two electrons in a double dot (of 30-nm radii) separated by 30 nm. Results of three different barrier heights are shown. The exchange coupling depends sensitively on the central barrier height.
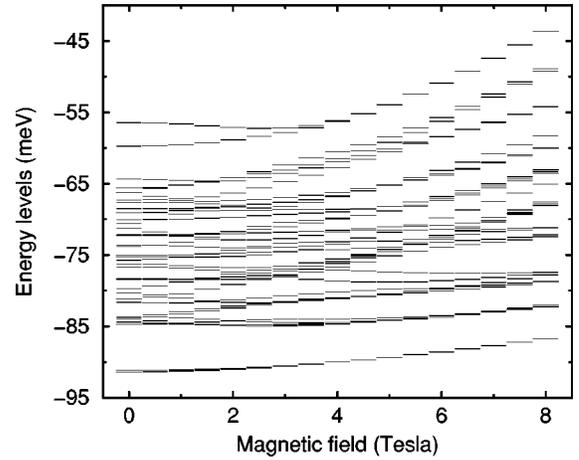

FIG. 5. Here we show the magnetic-field dependence of the energy spectra in a molecular-orbital calculation where both s and p single-electron orbitals are used. The interdot distance is 30 nm, and the central barrier V_b is 30 meV, corresponding to an actual barrier height of 9.61 meV.

Our Hund-Mulliken calculation (with only the electron s orbitals) results are shown in Fig. 4. Here we first perform a variational calculation at zero magnetic field. We vary the parabolicity and the location of the fitting parabolic well to achieve the lowest energy in the ground state. The results of the variational calculation are shown in Table I. For these optimal variational parameters the triplet state (the first excited state at zero and low magnetic field) is also quite close to its lowest energy. According to Fig. 4, the exchange coupling, or equivalently the singlet-triplet splitting, is a sensitive function of the central barrier height. This implies that a suitable gate-controlled central barrier can, in principle, be utilized to switch the exchange coupling on or off efficiently, thereby making possible two-qubit operations in our quantum-dot QC architecture. The magnitude of the exchange coupling ranges from 0.2 meV to about 1 meV in these structures, which correspond to gating times on the order of one picosecond to tens of picoseconds, which is difficult, but not impossible, to achieve.

The results of the molecular-orbital calculation done on the larger basis (including both single particle s and p orbitals) are shown in Figs. 5–7. Comparing this more sophisticated s-p-hybridized calculation, which includes the first ex-cited ''atomic'' orbitals, with the simple Hund-Mulliken calculation discussed above, we find that there is a significant effect arising from the strong mixing in of the higher excited states. In other words, s-p hybridization significantly lowers the energy of the lowest singlet state. Although the s-p-hybridized ground-state resemble the Heitler-London wave functions, it also contains components in which one electron is in one of the excited states. Such a contribution could be favorable for the quantum-dot molecule because p orbitals increase the ''bonding'' between the two quantum dots, thus lowering the overall energy of the double-dot system. In addition, our confinement potential is not exactly a sum of two symmetric parabolic wells. Instead, the two Gaussian wells and one Gaussian barrier complicate the contour of confinement, so that the true ground state has components of single-particle excited states of the fixed harmonic well potentials.

According to the calculated energy spectra shown in Fig. 5, the ground singlet and triplet states are well separated from the rest of the higher excited states in the Hilbert space. For the representative sample parameters as chosen, the higher excited states are always separated from the ground singlet-triplet states by at least 6 meV, which is much larger

TABLE I. Here we tabulate the variational parameters for the three different central barrier heights at a 30-nm interdot distance. The fitting well refers to the isotropic parabolic wells we use to fit the two Gaussian wells. We obtain the base parabolicity from the second derivative at the bottom of the confinement potential wells, and the base locations are the actual minima of the confinement potential wells.

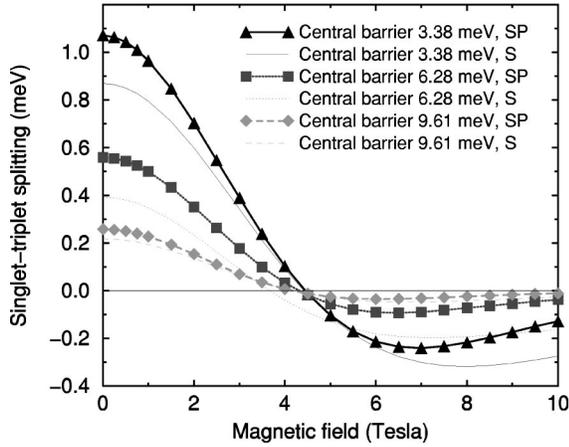|			
Central potential barrier V_b (meV)	20	25	30
Actual central barrier height (meV)	3.38	6.28	9.61
Change in parabolicity (meV)	-2.8281	-2.3915	-2.0044
Actual single particle excitation Energy at zero **B** field (meV)	8.4134	8.8499	9.2371
Change in fitting well location (nm)	-0.2243	-0.3779	-0.1632
Actual fitting well location At zero **B** field (nm)	12.6343	14.2441	16.0822

FIG. 6. Here we show the magnetic-field dependence of the exchange coupling in a molecular-orbital calculation with both *s* and *p* single-electron orbitals. The interdot distance is 30 nm. Results of three different barrier heights are shown, together with the results (in thin lines) from the Hund-Mulliken calculation for comparison. The exchange couplings from the full calculation are about 20% larger at zero magnetic field than those obtained from the Hund-Mulliken calculation.

than the maximum value of the exchange coupling, J (0.3 meV) as well as being much higher than $k_B T \lesssim 0.1$ meV at the cryogenic temperature of QC operation. Thus, as long as the coupling between the two quantum dots is turned on slowly, the two-spin two-electron system is quite isolated from the other parts of the Hilbert space, and is thus a good candidate for a quantum gate. This demonstration of a well-defined two-spin singlet-triplet Hilbert space, which is well separated from the rest of the higher excited states of the two-electron double-dot system, is one of the most important results of our work.
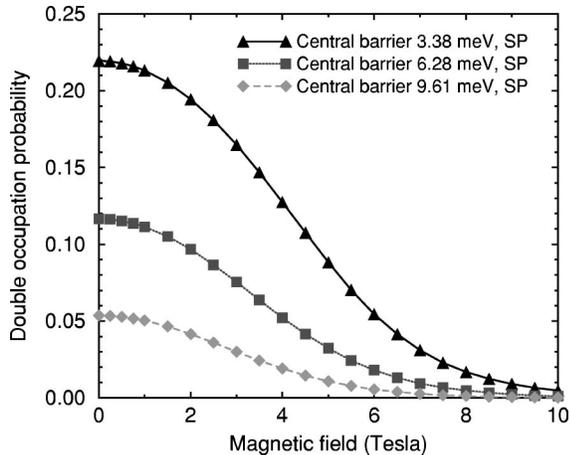

FIG. 7. Here we show the magnetic-field dependence of the double occupation probability in a molecular-orbital calculation with both *s* and *p* single-electron orbitals. This probability characterizes the double occupation occurring in the single-electron ground state of the left dot. It is clear that the two lower barrier cases, with their large double occupation probabilities, are not appropriate for the purpose of quantum computing at small magnetic fields.

Figure 5 also shows that there are discernible shell structures in the two-electron excitation spectra, and this structure changes with the magnetic field. The shell structure is especially prominent at large **B** field. The origin of the shell structure is apparently the degeneracy of the single particle Fock-Darwin states. At small **B** field, the wave function overlap between the two quantum dots is quite significant, so that the direct Coulomb repulsion and the exchange energy play important roles in deciding the energies of individual states. As the **B** field increases, the state overlaps between two quantum dots decrease since the wave functions are squeezed by the applied magnetic field, and consequently the Coulomb correlation between the two dots becomes less important (even though the on-site Coulomb repulsion becomes more important). The whole spectrum should then resemble that of two isolated single quantum dots. Another effect that should be taken into consideration is that for $|\mathbf{B}|>0$ the degeneracies of the Fock-Darwin states are lifted, so the single particle energy levels are scrambled. However, at certain specific magnetic-field values shells appear as several energy levels move close to each other and away from the rest. There are also apparent level crossings in the spectra, as the energies of individual Fock-Darwin states with different angular momenta change differently with the **B** field, and singlet and triplet states are not coupled by the Hamiltonian we consider. In summary, any simple magnetic-field dependence of the Fock-Darwin states is scrambled by the nonparabolic confinement potential and the varying Coulomb interaction between the two electrons. Although the origin of the shell structure is clearly the starting degeneracy of the Fock-Darwin levels, its detailed magnetic-field dependence is quite complex. The shell structure may, in principle, be useful for the purpose of quantum computing because a full shell plus one electron might be effectively considered as a spin-$\frac{1}{2}$ single-electron system, i.e., a filled shell could be considered ''inert.'' Whether such an effective spin-$\frac{1}{2}$ system with filled shells is sufficient as a qubit can only be demonstrated by a multielectron CI calculation of its spectrum, and clearly requires further investigation. Our molecular-orbital results in the presence of the external magnetic field could be considered suggestive of such a possibility.

Figure 6 shows the magnetic-field dependence of the exchange coupling (singlet-triplet splitting) with three different central barrier heights. Here we can see that all the thick curves (from the larger basis calculations) are shifted upwards from the thinner curves (from the smaller basis calculations). The reason for this change is that the larger basis allows us to obtain a much lower (and presumably more accurate) energy for the singlet states. The triplet states do not change nearly as strongly as the singlet states. Thus the exchange coupling J changes (increases) by 23%, 42%, and 18%, respectively, for 3.38-, 6.28-, and 9.61-meV central barriers in the more sophisticated calculations using the larger s-p-hybridized molecular-orbital basis. Note that the improvement in the calculated J is less for larger central barrier potentials. This is consistent with our belief that the p orbitals play a more important role when the two-dot overlap is larger, and therefore s-p hybridization effects are quantitatively more important when the interdot overlap (and hence

the exchange coupling) is larger.

Figure 7 shows the ground-state double occupation probability as a function of the magnetic field, which clearly decreases as the **B** field increases. The reason for this decrease with increasing magnetic field is straightforward. As **B** increases, the single-electron atomic wave functions become narrower. Thus the ''on-site'' Coulomb repulsion energy for the doubly occupied state increases rapidly, which decreases the double occupation probability. The ground-state double occupation probability can also be seen in Fig. 7 to decrease significantly with increasing central barrier strength separating the two dots (as one would expect). Here we do not show double occupation for the triplet state, because in those states one electron would have to be in an excited state; thus the probability is quite small, and could be considered negligible for most purposes in contrast to the ground singlet state situation shown in Fig. 7. The double occupation probability is an important parameter for a quantum-dot quantum computer (QDQC). In a QDQC, electron spins are qubits, while their residence quantum dots (QD's) (i.e., the individual dots on which the electrons are located) are their tags to distinguish the different qubits. If during the gating action two electrons jump onto a single QD due to high double occupation probability, even if they separate eventually, their original tag information is lost, which will result in an error requiring appropriate error correction. Thus, in designing a QDQC, one needs to minimize the double occupation probability for the states (especially the lowest singlet state) that belong to the QDQC Hilbert space. Indeed, Fig. 7 shows that for lower-barrier cases the double occupation probabilities are prohibitively large for the purpose of quantum computing. On the other hand, one cannot have a QDQC with very large central barrier (thereby producing very small double occupation probability) because then the exchange coupling (Fig. 6) will be very small, making two-qubit operations impossible. This indicates that one has to settle for a compromise in the pursuit of a large exchange coupling (for achieving smaller gating time during two-qubit operations) and a small double occupation probability (for reducing the error correction requirement).

To look for parameters that can lead to small double occupation probability but still maintain a finite exchange coupling for a double quantum dot, we increase the interdot distance from 30 nm as studied above to 40 nm and perform the molecular-orbital calculations. The results are shown in Figs. 8–11.

Again, we first vary the location and parabolicity of the fitting parabolic wells. In Fig. 8 we plot these variational parameters as functions of the central barrier height. One interesting feature shown in panel (a) of the figure is that the fitting well parabolicity increases as the central barrier height increases. In other words, when the barrier is low, the electron wave functions tend to be more spread out. Furthermore, panel (b) of Fig. 8 shows that the distance of the two fitting wells are closer when the central barrier is low. These results show that the two-electron artificial molecule is bounded tighter when the interdot barrier is low, in analogy to a diatomic molecule and its orbital contraction.

In Figs. 9 and 10 we show the magnetic-field dependence of the exchange coupling and the double occupation prob-
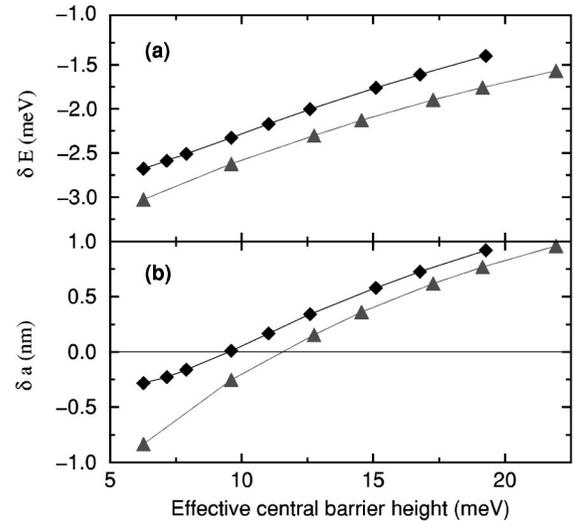

FIG. 8. Here we show the central barrier height dependence of the variational parameters in our study when the interdot distance is 40 nm. Panel (a) shows the change δE in the fitting well parabolicity, while panel (b) shows the change δa in the locations of the two fitting wells (symmetric about the origin). The decrease in parabolicity and interorbital distance indicates an analogy to orbital contraction and bonding in molecular physics.

ability. The values of both these quantities at zero magnetic field are about half of their values in Figs. 6 and 7 (with the same barrier heights). Therefore, at zero magnetic field, the exchange coupling and double occupation probability decrease at about the same rate as we pull the two quantum dots away from each other. In Fig. 11 we also plot the central barrier height dependence of both the exchange coupling and the double occupation probability. Both quantities decrease
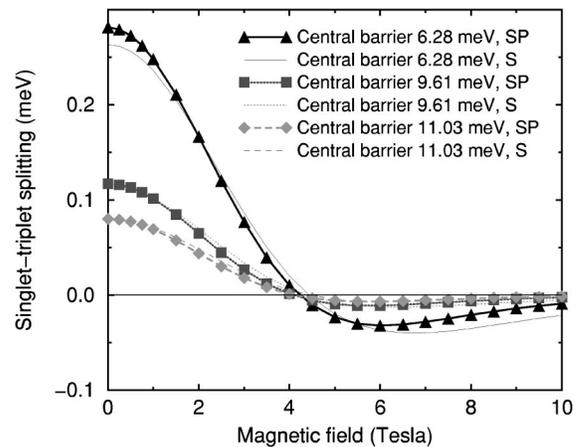

FIG. 9. Here we show the magnetic-field dependence of the exchange coupling in a molecular-orbital calculation using both s and p single-electron orbitals. The interdot distance is 40 nm. Results of three different barrier heights are shown, together with the results (in thin lines) from the Hund-Mulliken calculation for comparison. The exchange couplings from the full calculation are only slightly larger at zero magnetic field than those obtained from the Hund-Mulliken calculation, but there are some differences at finite magnetic fields.
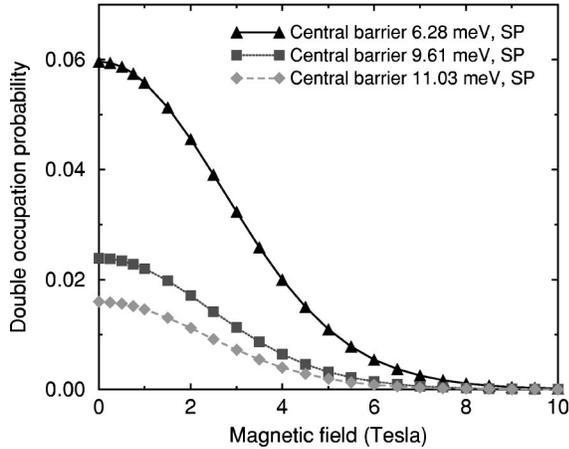
FIG. 10. Here we show the magnetic-field dependence of the double occupation probability in a molecular-orbital calculation with both s and p single-electron orbitals. The interdot distance is 40 nm. This probability characterizes the double occupation occurring in the single-electron ground state of the left dot. At high magnetic fields the double occupation probabilities are vanishingly small for all three cases.

exponentially as we increase the central barrier, as one expects. In the range of the barrier heights we considered, the exchange coupling decreases from 0.27 to 0.0097 meV, a change of about 28 times; the double occupation probability decreases from 0.060 to 0.0017, a change of about 35 times. Although the double occupation probability decreases a little faster than the exchange coupling, the difference is insignificant. Thus we also show that these two quantities change at about the same rate as we change the central barrier height.
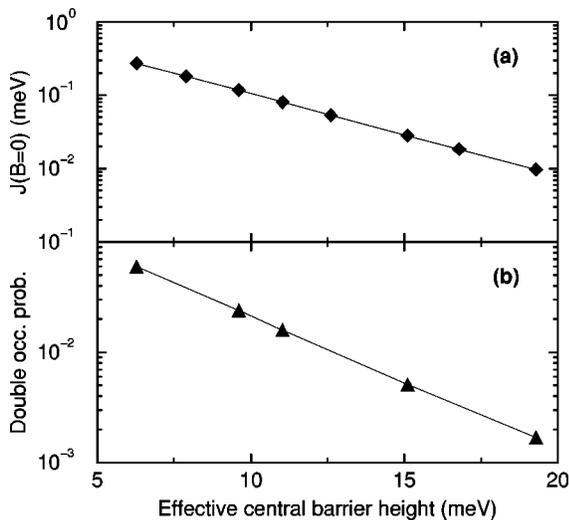

FIG. 11. Here we show the central barrier height dependence of the exchange coupling J and the double occupation probability at zero magnetic field. The interdot distance here is 40 nm. Both quantities decrease exponentially as functions of the central barrier height. The rates of these decreases for both quantities are about the same. As the central barrier height varies in the shown range, J changes from 0.27 to 0.0097 meV, while the double occupation probability changes from 6% to 0.17%.

Therefore, at zero magnetic field, it would be difficult to achieve a vanishingly small double occupation probability while maintaining a sizable exchange coupling.

However, as shown in Figs. 9 and 10 (and also Figs. 6 and 7), a finite magnetic field may lead to a solution to this problem of correlated exchange coupling and double occupation probability. Physically, the exchange coupling is determined by the competition between direct and exchange Coulomb interactions, while the double occupation probability is mainly determined by the direct Coulomb repulsion. It is thus expected that the two quantities have different dependence on the magnetic field. Indeed, according to Figs. 6, 7, 9, and 10, for magnetic field above 6 T the magnitude of the exchange coupling decreases quasilinearly, while the double occupation probability decreases exponentially fast. For example, in Fig. 10, at a magnetic field of 7 T and an effective central barrier of 9.61 meV, the double occupation probability is about 6×10^{-4}, a magnitude that is of the same order as the tolerance of the currently available error correction codes, while the exchange coupling in this case is about 0.009 meV, corresponding to a swap gate time of about 3 ns (after taking into account adiabaticity). Thus the difference in the magnetic-field dependence of the exchange coupling and the double occupation probability can be exploited for optimal QC operations. This is another important result of our calculation in the context of QDQC architecture.

V. DISCUSSIONS

A. Validity of the envelope-function approach

The issue of the adequacy of the single-envelope-function effective-mass approximation (used throughout our calculations) for the purpose of studying electron entanglement in the context of a QDQC requires careful consideration. Let us first discuss the validity of the envelope-function approach in our study of the electronic structure of a 2D GaAs-based double-dot molecule. One necessary condition [41] is that the $\mathbf{k} \cdot \mathbf{p}$ approximation should be valid in our problem. For the GaAs conduction band, the $\mathbf{k} \cdot \mathbf{p}$ approximation (''Kane model'') is valid up to $\epsilon_{\mathbf{k}} - \epsilon_0 \sim 0.3$ eV, where ϵ_0 is the conduction-band edge energy and $\epsilon_{\mathbf{k}}$ is the energy of a conduction electron at momentum $\mathbf{k}$ in the Brillouin zone. In our study of the coupled-quantum-dot molecule, the energy scale of the electrons is in the order of 10 meV, making the $\mathbf{k} \cdot \mathbf{p}$ approximation valid.

Another condition for the validity of the envelope function approach is weak intervalley scattering. The electronic wave functions in this paper are built from conduction-band Γ-point Bloch functions. However, if a GaAs quantum well (in the growth direction we have a narrow GaAs quantum well sandwiched between $Al_x Ga_{1-x} As$ barriers) is too narrow (<3 nm), the X valley would lie close to the Γ point in energy, so that a more complete approach (going beyond the single-envelope-function approach) is needed to take into account the Γ-X intervalley scattering. An envelope function approach becomes inappropriate because it only *locally* describes a small part of the Brillouin zone. Thus, for our approach to be valid, the quantum well in the growth direction cannot be too narrow [41]. Calculations going beyond the

single envelope approximation for GaAs quantum wells, however, show [41] that even for such extremely narrow quantum wells, the single envelope function approximation gives qualitatively (and semiquantitatively) accurate results.

Although we do not think it to be necessary at present, one can go beyond the single-envelope-function approximation. A more complete analysis (than our single-envelope-function model) would employ an 8×8 Kane model [41] to include all the closeby valence bands, with two Γ_6 states corresponding to the conduction bands, four Γ_8 states corresponding to the heavy- and light-hole bands, and two Γ_7 states corresponding to the split-off band. We would then have eight envelope functions instead of just one as we use here. The complete single-electron Schrödinger equation and the general QD Hamiltonian without any magnetic field take the forms

$$H \psi = E \psi,$$

$$H = \frac{\mathbf{p}^2}{2m_0} + U(\mathbf{r}) + V(\mathbf{r}_\perp), \qquad (8)$$

$$\psi = \sum_{i=1}^{8} f_i u_{i0}.$$

Here m_0 is the bare electron mass. $U(\mathbf{r})$ is the crystalline periodic potential, which assumes different values in the quantum well and in the barriers. It thus has a steplike overall profile along the z direction. $V(\mathbf{r}_\perp)$ is the QD confinement potential produced by an external static electric field arising from lithographic gates, dopants, and all other sources not contained in $U(\mathbf{r})$. $\mathbf{r}_\perp$ refers to the 2D x-y plane, i.e., directions perpendicular to the z direction. Since the z-direction confinement is very narrow while V is slowly varying, we neglect its variation along the z direction. u_{i0}'s are the Γ-point Bloch functions, which are the same as the atomic orbitals of the constituent elements. f_i's are the eight envelope functions corresponding to the eight relevant bands, which are slowly varying functions on the atomic scale. The Schrödinger equation can be simplified into a set of equations for the envelope functions f_i's by using the following identity:

$$\int_\Omega f(\mathbf{r}) u(\mathbf{r}) d\mathbf{r} \cong \frac{1}{\Omega} \int_\Omega u(\mathbf{r}) d\mathbf{r} \int_\Omega f(\mathbf{r}) d\mathbf{r}$$

$$= \frac{1}{\Omega_0} \int_{\Omega_0} u(\mathbf{r}) d\mathbf{r} \int_\Omega f(\mathbf{r}) d\mathbf{r}. \qquad (9)$$

Here Ω is the total volume of the crystal, Ω_0 is the volume of one unit cell, $f(\mathbf{r})$ is a slowly varying function on the atomic scale, and $u(\mathbf{r})$ is a fast varying and periodic function on the atomic scale. This identity can be proved by assuming that $f(\mathbf{r})$ is a constant in each unit cell of the crystal. The set of equations for the envelope functions is then (assuming an $Al_x Ga_{1-x}As$-GaAs-$Al_x Ga_{1-x}As$-type heterostructure in the z direction, with A/B below denoting $Al_x Ga_{1-x}As$-GaAs)

$$\sum_m \left\{ \left[\frac{\mathbf{p}^2}{2m_0} + [\epsilon_l^A Y_1 + \epsilon_l^B Y_2 + \epsilon_l^A Y_3 + V(\mathbf{r}_\perp)] \right] \right.$$
$$\left. \times \delta_{lm} + (\boldsymbol{\pi} \cdot \mathbf{p})_{lm} \right\} f_m(\mathbf{r}_\perp, z) = E f_l(\mathbf{r}_\perp, z). \qquad (10)$$

Here ϵ_l^A and ϵ_l^B are band edge energies of materials A and B at the lth band edge at Γ point. Y_i are step functions that take the value 1 for the ith layer and 0 everywhere else—we assume sharp interfaces between materials A and B (although deviations from sharpness can be built into the model). $\boldsymbol{\pi}$ is the interband transition matrix, which is essentially the expectation value of momentum operator $\mathbf{p}$ in a unit cell. We can separate f into an in-plane 2D component and a z-direction component, and further simplify the equations. In addition, the valence-band envelope functions can be written in terms of the two conduction-band functions, thus leading to a *nonlinear* (but only 2×2) eigenvalue problem. The presence of a slowly varying electric field (for the purpose of confinement) plus the band edges for the heterostructure introduces additional (on top of interband coupling in bulk GaAs) coupling between different bands [41]. At the zeroth-order approximation, when one neglects all spin-orbit coupling terms and interband couplings, the set of equations above reduces to the single-envelope-function Schrödinger equation we employ in our current study. In our approximation the only effects of the band structure are to replace the bare electron mass m_0 by an effective mass m^* and the bare Coulomb interaction by its screened form, which is precisely the single-envelope-function effective-mass approximation.

To validate our zeroth-order approximation, we need to estimate the magnitudes of the higher-order corrections neglected in our approximation. In particular, we can evaluate the quantity $p = E_p \bar{E} m^* / m_0 E_g^2$ [41], where p is the strength of the interband and spin-orbit corrections relative to the zeroth-order terms within each conduction band. Here E_p represents the interband coupling strength, $\bar{E}$ is the characteristic electron envelope energy, m_0 is the bare electron mass, m^* is the conduction-band effective mass, and E_g is the fundamental band gap at the Γ point. For GaAs, $E_p = 22.71$ eV, $m^* = 0.067 m_0$, $E_g = 1.5192$ eV [41], and the characteristic electron energy $\bar{E}$ is about 10 meV. Using these parameters, we obtain $p \sim 1/150$, which is indeed a small quantity, justifying our envelope-function effective mass approximation in the low-energy singlet-triplet sector. The off-diagonal corrections, which couple the spin-up and -down components of the envelope wave functions, have similar negligibly small magnitudes. For the spin-coupling the corresponding small parameter is $p' = E_p \Delta \bar{V} m^* / m_0 E_g^3$, where Δ is the valence-band splitting due to spin-orbit coupling and $\bar{V}$ is the average confinement energy. For GaAs $\Delta = 0.341$ eV, while we take $\bar{V} \sim 50$ meV. We then obtain $p' \sim p \sim 1/150$. Therefore, up to an accuracy of 1%, the conduction bands of two different spins are decoupled from each other and from other valence bands, and the use of a single-band envelope function may be quite useful qualitatively and semiquantitatively. It would, however, require further nu-

merical investigations going beyond the single-envelope-function approximation to establish whether this accuracy is consistent with the stringent error correction requirements in a QC.

To go beyond the zeroth-order approximation, the above-mentioned correction terms need to be included, and the linear Schrödinger equation we have now becomes a nonlinear eigenvalue problem, with a nonvanishing off-diagonal term that couples the up- and down-spins. Thus, strictly speaking, because of spin-orbit coupling, the spin-up and -down states of a conduction electron are not the eigenstates in a semiconductor heterostructure. This opens another possible, albeit weak, channel for spin decoherence in quantum dots that is not present in the bulk.

When a magnetic field is introduced, it can be directly incorporated in the envelope-function effective Hamiltonian. The underlying Γ-point Bloch functions, which are atomic wave functions, are only minimally affected by the external magnetic field. Indeed, in a typical atom, the $\mathbf{A}^2$ term is about 10^{-3} as large as the linear term in a 10-T field, which can be safely neglected. The linear term in $\mathbf{A}$ corresponds to the coupling between the electron orbital angular momentum with the external magnetic field. For the S orbital of the conduction band, this coupling vanishes; for the P orbitals of the valence bands, the magnitude of the splitting caused by this term is about 1 meV per 18 T. Compared to the main gap of about 1.5 eV, this splitting can also be safely dropped. Therefore, we can conclude that the underlying Bloch functions are not affected by any moderate (up to 10 T) external magnetic fields one needs for QDQC operation. We also conclude that for the purpose of QDQC operations, where one restricts to only the low energy singlet-triplet sector of the Hilbert space, the single-envelope-function effective-mass approximation employed in this paper is qualitatively excellent, but further studies are needed to establish whether this approximation satisfies the demanding constraints of error correction in a realistic QDQC architecture.

B. Singlet-triplet crossing

In our calculations we find a singlet-triplet crossing in all the situations we considered for a magnetic field around 4 T. The physical reason underlying this magnetic-field-induced singlet-triplet crossing (making the triplet state the ground state in high fields) is somewhat subtle. In a single-quantum-dot ''helium atom'' (two electrons in one dot), where such a crossing has also been reported in the literature, the competition between interelectron Coulomb repulsion and single-particle excitation is the reason for the singlet-triplet crossing [22,44]. In the quantum-dot hydrogen molecule that we consider (two electrons in two dots), the electrons can reside in different dots, minimizing the Coulomb repulsion effect, and therefore the above reasoning does not really apply for our singlet-triplet crossing. To achieve a better understanding of this crossing, we first write down the expression for the singlet-triplet energy splitting (exchange coupling) using the Heitler-London wave functions of the ground singlet and triplet states:

$$|\Psi_s\rangle = \left[\frac{|\phi_L(1)\rangle|\phi_R(2)\rangle + |\phi_L(2)\rangle|\phi_R(1)\rangle}{\sqrt{2}}\right]\frac{|\uparrow\downarrow\rangle - |\downarrow\uparrow\rangle}{\sqrt{2}},$$
(11)

$$|\Psi_t\rangle = \left[\frac{|\phi_L(1)\rangle|\phi_R(2)\rangle - |\phi_L(2)\rangle|\phi_R(1)\rangle}{\sqrt{2}}\right]\frac{|\uparrow\downarrow\rangle + |\downarrow\uparrow\rangle}{\sqrt{2}},$$

where $|\phi_L\rangle$ and $|\phi_R\rangle$ are localized electron spatial orbitals. The exchange coupling—the energy splitting between the lowest triplet and singlet states—can then be expressed as

$$J = \frac{\langle\Psi_t|H|\Psi_t\rangle}{\langle\Psi_t|\Psi_t\rangle} - \frac{\langle\Psi_s|H|\Psi_s\rangle}{\langle\Psi_s|\Psi_s\rangle} = J_r + J_c,$$
(12)

where J_r is the contribution from the single-particle potential energy, while J_c is the contribution from Coulomb interaction between the two electrons. J_r and J_c can be expressed as

$$J_r = \frac{2|S_{LR}|^2}{1-|S_{LR}|^4}[\langle\phi_L|\Delta V_L|\phi_L\rangle + \langle\phi_R|\Delta V_R|\phi_R\rangle$$
$$- \langle\phi_R|\Delta V_L|\phi_L\rangle - \langle\phi_L|\Delta V_R|\phi_R\rangle],$$
(13)

$$J_c = \frac{2|S_{LR}|^2}{1-|S_{LR}|^4}\left[\langle\phi_L(1)\phi_R(2)|e^2/\epsilon r_{12}|\phi_L(1)\phi_R(2)\rangle \right.$$
$$\left. - \frac{\mathrm{Re}\langle\phi_L(1)\phi_R(2)|e^2/\epsilon r_{12}|\phi_L(1)\phi_R(2)\rangle}{|S_{LR}|^2}\right],$$

where $S_{LR} = \langle\phi_L|\phi_R\rangle$, $\Delta V_L = V(x,y) - V_L$, and $\Delta V_R = V(x,y) - V_R$, with $V(x,y) \equiv V(\mathbf{r}_i)$ of Eq. (1). Here V_L is a harmonic well located on the left and V_R is a harmonic well located on the right. The basis wave functions ϕ_L and ϕ_R are eigenstates of these two wells, respectively. Thus we can see that J_r is a contribution due to the difference caused by replacing the actual confinement potential V by a left or right harmonic well. It is a single-particle contribution. Whether J_r is positive or negative depends on the particular choice of V and the parabolicity choice for V_L and V_R. When the distance between the two quantum dots becomes large, this quantity approaches zero.

The Coulomb contribution J_c consists of two parts, one from direct Coulomb interaction, the other from exchange interaction. These two parts generally do not have the same type of dependence on an external magnetic field $\mathbf{B}$. As $\mathbf{B}$ increases in strength, the exchange interaction becomes more important, which leads to singlet-triplet crossing in a quantum dot molecule. An analytical calculation for a special (somewhat artificial) confinement potential was recently performed [39], which explicitly demonstrated the different behavior of the direct Coulomb and exchange terms.

The expression for J shows that there are multiple contributions to the energy difference between singlet and triplet states. Without analytical expressions it is difficult to determine exactly which factor dominates in a particular range of parameters. Physically, the Pauli principle constraint deter-

mines that in a triplet state the two electrons will try to avoid each other, thus establishing a repulsive correlation between them. This correlation helps to lower the Coulomb interaction energy, favoring the triplet state to have a lower energy if Coulomb interaction is dominant. As the external magnetic field is increased, the wave-function overlap decreases because of the squeezing by the magnetic field, so the long-range Coulomb interaction becomes the dominant factor in the total two-electron interaction energy, leading to the triplet state being the ground state at high enough magnetic fields. On the other hand, at lower magnetic fields, the wave-function overlap is significant; a singlet state is then the ground state since it lowers the electron kinetic energy. A singlet-triplet crossing is therefore inevitable as a function of the magnetic field, which for the double-dot parameters we choose, happens at rather low accessible fields of 4 T.

C. Quantum-chemical approaches

As we mentioned above, the Schrödinger equation for a two-center two-electron problem cannot be solved exactly. Various quantum-chemical approximations have been proposed and implemented in this problem in the context of electronic energy-level calculations in real molecules [40]. Below we present a summary and a critique of the various techniques which may be useful in the calculations for obtaining realistic QDQC architectural parameters. Since the exact electron wave functions are important in the context of quantum computing, we will not discuss approaches that deal only with electron charge or spin densities. We believe that detailed electronic structure calculations, which provide accurate information about the wave functions spanning the relevant Hilbert space for realistic QDQC architecture, will be absolutely essential for further progress in this field.

1. Hartree-Fock approximation

One of the simplest quantum-chemical approaches is the Hartree-Fock approximation. It uses an effective single-electron equation to simulate a two-electron problem. The Pauli principle is accounted for because the two-electron wave function is written as a single Slater determinant. The HF equation can be solved directly or on a finite basis (the so-called linear combination of atomic orbitals method). The main advantages of a HF calculation are its single-particle feature, its accessibility, and its clear underlying physical picture. The main shortcoming is its disregard of electron correlations, which originates from the simplification of a two-particle problem to a one-particle problem. This deficiency can be systematically remedied by introducing configuration interaction (CI) corrections. Instead of using a single Slater determinant as the system wave function, one can use a series of Slater determinants (in which the single-particle wave functions are HF wave functions including the excited states) as basis and search for the best combination. As the size of this basis goes to infinity, the method becomes exact. One may, however, be able to obtain a very high accuracy with a reasonable size CI calculation if the configurations to be mixed in are chosen judiciously.

One potential shortcoming of the Hartree-Fock method for the purpose of quantum computation is that it may not be sufficient to describe quantum entanglement. Multielectron wave functions are intrinsically inseparable when there are overlaps between single-electron wave functions. As a consequence of electrons being *indistinguishable*, a Slater determinant is not a simple separable product function, and therefore individual electron states generally cannot be factored. For example, consider a two-particle Slater determinant

$$|\Psi\rangle = \frac{1}{\sqrt{2}}[|\phi(1)\rangle|\uparrow\rangle_1|\psi(2)\rangle|\downarrow\rangle_2$$
$$-|\phi(2)\rangle|\uparrow\rangle_2|\psi(1)\rangle|\downarrow\rangle_1]. \quad (14)$$

We can easily calculate the single-particle density matrix for particle 1,

$$\rho_1 = \mathrm{Tr}_2(\rho_{12})$$
$$= \mathrm{Tr}_2(|\Psi\rangle\langle\Psi|)$$
$$= \frac{1}{2}[|\phi(1)\rangle\langle\phi(1)||\uparrow\rangle_1\langle\uparrow|_1$$
$$+ |\psi(1)\rangle\langle\psi(1)||\downarrow\rangle_1\langle\downarrow|_1], \quad (15)$$

which is indeed a mixed state. However, this inseparability in the Slater determinant arises only from correlations due to the Pauli exclusion principle. If the electrons are spatially separated so that they become *distinguishable*, the electron wave function of Eq. (14) becomes a product. For example, if ϕ and ψ above are localized spatially with no overlap, the above two-particle wave function simplifies to

$$|\Psi\rangle = |\phi(1)\rangle|\uparrow\rangle_1|\psi(2)\rangle|\downarrow\rangle_2. \quad (16)$$

Here 1 and 2 are labels of the two distinguishable particles—particle 1 in ϕ and particle 2 in ψ. The two-electron wave function is now in a product form, and the state for each particle is pure. In other words, Eq. (16) is not an entangled state.

In the RHF approach, the spin part of the wave function would be a singlet for two electrons when they occupy the same spatial orbital, so that the state is necessarily entangled. The entanglement here is fundamentally different from the inseparability that arises purely out of the Pauli exclusion principle as considered above. Instead, it represents a true correlation between the two particles—they occupy the same spatial orbital. On the other hand, in the UHF approach the wave function is completely separable when the two wave functions are localized, so that no entanglement can be described. In general, for indistinguishable particles, the entanglement information is encoded in the form of superposition of different Slater determinants so that, in principle, CI is always *needed* for the wave function to carry entanglement information. From another perspective, for n spin-$\frac{1}{2}$ particles, the number of real variables needed to describe the spin part of the entangled multielectron wave function is $2^{n+1} - 2$, while one Slater determinant only provides $2n$ real variables to describe the spin degrees of freedom, which is clearly not

enough to incorporate entanglement in any multielectron case, including even the $n=2$ two-electron case we consider here. Therefore, the single Slater determinant HF approximation is manifestly inadequate for QC purposes. One should note, however, that the HF approximation is not intended for the purpose of describing quantum entanglement. It is designed to compute accurately electronic energy spectra, charge and spin densities, etc. Therefore, as long as one recognizes the shortcomings of this method, it can still provide valuable information about the electronic system.

2. Heitler-London method

A Hartree-Fock calculation is self-consistent, and in it a mean field is produced by the calculated electron density. One can also solve the two-electron problem using a fixed finite molecular-orbital basis. Indeed, when the number of states in the basis goes to infinity, the solution approaches an exact two-electron state. However, the convergence may be slower than a self-consistent calculation (with CI), and it quickly becomes computationally intractable for multielectron problems. On the other hand, for a two-electron problem with a small number of basis states, such a fixed finite-basis calculation is numerically tractable and provides a clear advantage over the HF approximation for studying entanglement.

The Heitler-London method is an approximation of the simplest molecular-orbital calculation. Here only the two single-particle ground states in the individual quantum dots are taken into account. Furthermore, in forming two-electron orbitals, the two ''polar'' (doubly occupied) states are neglected. There is then only one possible functional form each for singlet and triplet states, respectively. This approach is quite accurate when the two dots are far from each other, so that the single-particle wave functions have the correct dependence on the interdot distance. On the other hand, if the two dots are brought close to each other, the wave functions' radii should be varied in order to obtain the lowest energy for the two-electron states. This is similar to the orbital contraction in molecular physics when two binding atoms are brought together [40], although in quantum dots it might be orbital expansion rather than contraction. Another way to improve Heitler-London calculation is to introduce orbital ''polarization'' (a contortion of the s orbitals toward each other), so that anisotropies in the problem can be at least partly accounted for. For example, p orbitals can be included in the single-particle wave functions (s-p hybridization) [39]. Indeed, in the case we considered in this paper, s-p hybridization is an extremely important feature of the problem, as we already discussed in Secs. III and IV of the paper.

3. Molecular-orbital theory

The Heitler-London method is appealing in its simplicity and its clear physical picture. However, unless perfect basis states happen to be ''luckily'' chosen, it is difficult for a method with such a small basis to accurately describe a double-dot molecular system. The first improvement one can make is to include the polar states. It then becomes the simplest molecular-orbital calculation—the Hund-Mulliken approach [39]. To further enlarge the basis, one just includes more single-particle orbitals. For example, in our case, we have included all the single-particle first-excited states, so that there are in total six single-particle states forming our basis, from which we can form 36 two-particle states. If n single-particle orbitals are used, the number of two-particle states grows as n^2, while the number of Coulomb matrix elements grows as n^4. It is thus imperative to select the best possible single-particle wave functions, so that the number of these orbitals can be kept at a minimum, allowing a tractable computation.

To limit the size of the two-electron state basis, one can select a portion of states from a more complete basis, using criteria such as a single-particle energy cutoff. Such an approach amounts to a Heitler-London calculation supplemented by limited CI. However, there can always be hidden hazards in this practice. For example, as has been pointed out [45], the calculation of exchange energy is nontrivial in an array of atoms. One reason is that exchange is mainly determined by tail overlaps between neighboring electron wave functions, where Heitler-London wave functions (often used for calculating exchange energy) are less reliable. In addition, including more configurations and going beyond Heitler-London wave functions may not improve the accuracy because the excited atomic wave functions have different exponential tails. Thus the eigenstates may have more accurate shapes near the atomic cores, but their tails may become less accurate, leading to an inaccurate exchange coupling energy. Indeed, it is always a dangerous practice to obtain a small quantity numerically from the difference of two large quantities. In quantum-dot molecules, the tail behavior of wave functions is somewhat simpler than in atoms because all the harmonic well eigenfunctions have the same long-distance exponential behavior (but multiplied by different polynomials). Therefore, by including a larger basis and doing limited CI calculations, one should be able to achieve a reasonable description of the eigenstates, eigenenergies, and in particular, the exchange energy in QDQC architectures. In this particular sense, 2D harmonic confinement in QD systems may provide a significant calculational advantage over the corresponding real atom-molecule situations with Coulomb confinement. On the other hand, the nonsingular nature of the harmonic potential well also means that the electronic states are more sensitive to the actual details of the confinement, making the QDQC architecture a fragile one for quantum computation.

4. Hubbard model

The Hubbard model is a highly simplified model describing Coulomb correlation effects in an array of atoms. The model [46] deals with a second-quantized multielectron Hamiltonian with a cutoff in the interaction. Only one orbital state per site is kept (in the atomic limit), and there is a finite hopping term t, arising from overlap, between the neighboring orbitals. The long-range Coulomb interaction is replaced by a single on-site repulsion term U—the rationale being that screening by all the other electrons lead to an on-site effective U. The ferromagnetic direct exchange part of the Hamiltonian is dropped because the wave-function overlap be-

tween neighbors is exponentially small. Multisite Coulomb interaction is also neglected, assuming that they do not affect the magnetic properties of the model. In the limit of large on-site repulsion (large U), the effective Hamiltonian that describes the excitation of this model is a Heisenberg exchange Hamiltonian, with the exchange coupling J related to t and U by $J=4t^2/U$. As this J is always positive, the ground state is antiferromagnetic when there is one electron per site. There are various attempts to add additional terms to the Hubbard model (the extended Hubbard models) so that it can describe various other phenomena. For example, in one extended Hubbard model, nearest-neighbor Coulomb interaction is also taken into consideration. The model can then describe spatial charge-density fluctuations.

The Hubbard model and its variants have been applied to quantum-dot arrays [47], particularly in the context of transport and magnetic properties, and also to study quantum phase transitions in quantum-dot arrays. It is an effective model that can describe complex phenomena with simplicity. In the context of a QDQC, using spins as qubits it is unclear that the Hubbard model could have a considerable relevance because of its extreme simplicity. This is certainly true for the two-electron model in the double-dot problem studied in this paper. However, if multiple-dot algorithms are designed in the future, the Hubbard model may become a powerful tool, although various details will have to be added, diminishing the simplicity of the original model.

The Hubbard model reduces to the Heisenberg model in the large on-site repulsion limit ($U \rightarrow \infty$). One condition for the validity of the Heisenberg exchange Hamiltonian is that each localized electron wave function should have exponentially small overlaps with others. This condition is generally not satisfied in the QDQC when we bring two quantum dots very close to each other. However, for a two-electron problem, if the orbital degrees of freedom are frozen, the spin degree of freedom has only four dimensions which can be described by singlet and triplet states, and a Heisenberg model description becomes possible. On the other hand, if the electron orbital degrees of freedom are ever excited, the Heisenberg exchange Hamiltonian will not be applicable for our purpose. For example, if two electrons ever enter one quantum dot simultaneously, we will lose track of which qubit is represented by which spin; thus the error probability would be 50%. As we have shown previously, at low magnetic fields in the current configuration, the ground singlet state has a finite probability (as large as 20% or more at zero magnetic field) of double occupation in either dot. For a short QC calculation or for qualitative results, a 5% double occupation probability may be acceptable. However, this small error becomes a very serious problem that cannot be overcome by currently available error correction schemes for a long quantum computation, leading to the constraint that the double occupation probability must be kept very low.

D. Various aspects of a quantum-dot quantum computer

It has been pointed out that the spin-based quantum-dot quantum computer, in principle, satisfies the necessary and sufficient conditions required for quantum computing [14].

Here we would like to discuss in further detail a number of salient features that arise naturally in the context of a QDQC.

In many materials, electron spins are less vulnerable to decoherence than their orbital degrees of freedom, which in fact is the main motivation for the proposed spin-based QDQC. For example, carriers in GaAs have a subpicosecond momentum-relaxation time, while their spin-relaxation time is longer than 1 ns [43]. Since a long spin coherence time is absolutely essential for QDQC operations (in particular the spin coherence time must be much longer than the single- and two-qubit operation times, which have to be controlled by switching magnetic fields and gates, and cannot be very fast), we briefly summarize spin-relaxation mechanisms and comment on their relevance in the context of two-dimensional GaAs quantum-dot structures.

There are three major spin-relaxation channels for conduction electrons in GaAs: the Elliott-Yafet (EY) mechanism, the D'yakonov-Perel' (DP) mechanism, and the Bir-Aronov-Pikus (BAP) mechanism [19]. The EY process originates from the fact that real Bloch functions are not spin eigenstates. For example, spin-orbit coupling can mix spin-up and -down states in the electron eigenstates. Thus, whenever an electron is scattered (by other electrons, phonons, impurities, etc.), there is a finite probability that the dominant spin component will flip, thus causing spin relaxation. The DP channel arises from the lack of inversion symmetry in GaAs, which leads to an intrinsic spin splitting in the conduction band even for zero magnetic field. In the DP channel, the energy band splitting due to spin-orbit coupling is treated as an effective magnetic field. For different **k** states, this effective field has different magnitudes and directions. Thus, as an electron is scattered from one momentum state to another, it sees different fields and precesses differently whenever it is scattered. Soon the electron loses the memory of its initial spin state, thus showing spin relaxation. The BAP channel is somewhat similar to the DP channel, as it also treats electron spins as precessing in an effective magnetic field. However, in the BAP mechanism the effective field for the conduction electrons is produced by free or bound holes (or other paramagnetic impurities which may be present). Hole spins relax very quickly, so that the effective fields (the conduction electrons) produced by hole spins fluctuate, which causes an electron spin to lose information about its initial state.

In GaAs heterostructures, it is generally believed that the DP mechanism is the dominant spin-relaxation channel for conduction electrons [19]. In particular, due to the band discontinuity in a heterostructure, there is an additional spin splitting for the conduction electrons ("Rashba" effect) which can be treated as an extended DP channel. For holes, however, the EY mechanism is the dominant process. An additional complication is that in a quantum dot produced by modulating electric fields through lithographic gates, the confining electric field produces a mixing between the spin-up and -down states (in addition to the basic splitting arising from the lack of inversion symmetry in GaAs). The boundaries and the interfaces are also known to cause spin relaxation. Indeed, these additional spin-relaxation channels may actually be the dominant processes for electrons con-

fined in the quantum dots, because the wave functions for these electrons are built from the Γ-point Bloch functions, where the underlying Bloch function is S type, which has no spin-orbit coupling. Since the DP channel depends on the effective field produced by the spin-orbit coupling (which vanishes at the Γ point), and an external magnetic field may also help limit the DP channel, electron spin relaxation in a quantum dot should be quite weak (and probably arises primarily from the interface-boundary scattering, the confining electric field, and perhaps the Rashba effect).

When electron spin relaxation originating from the spin-orbit coupling (DP channel) is largely suppressed, other relaxation channels have to be carefully considered. In particular, interface-boundary-scattering-induced spin relaxation needs to be considered. In addition, it has been pointed out [39] that nuclear spins may affect electronic spin relaxation through the hyperfine interaction. This spin-relaxation channel can, however, be substantially suppressed by applying an external magnetic field or through the Overhauser effect to dynamically polarize the nuclear spins [39]. These issues require more careful (and quantitative) considerations before QDQC architecture questions can be seriously considered.

If the spin-orbit coupling is strong so that electron spin by itself is no longer a good quantum number, then one must consider the total angular momentum J, which involves both spin and orbital degrees of freedom. Such a mixing by itself would not be a disaster for quantum computing, since J can now replace electron spin to serve as the qubit. However, the ''spin'' relaxation time will then be in the same order of magnitude as the momentum relaxation time, which is generally very short ($\sim$ picoseconds or less) in semiconductors, which could be disastrous from the QC perspective. It is thus imperative to choose materials with small spin-orbit coupling for the purpose of electron-spin quantum computing—otherwise decoherence problem makes QC operations impossible.

Even if spin relaxation can be neglected (for example, because of long spin coherence time), there are many other factors that can affect the performance of a quantum computer. For example, based on our molecular-orbital calculation, the exchange coupling in a coupled-dot system is found to be large enough for fast picosecond switching. However, one has to be careful in exploiting the possibility of fast switching. Indeed, to produce the best structure for the purpose of quantum computing, a compromise needs to be achieved between an optimal gating time and an optimal error rate that should both be as small as possible. As we learned from our calculations and from general arguments, exchange coupling decreases exponentially quickly as the two dots are pulled apart. Consequently, to have a larger exchange coupling (which means a shorter gating time), the dots should preferably be close to each other, which, however, increases the overlap between the electron wave functions, leading to an enhanced double occupation probability, which means higher error rate. A compromise in the QDQC architecture will therefore be needed.

As shown in our molecular-orbital calculation, the subspace of the total Hilbert space containing the ground singlet and triplet states is well separated from the rest of the Hilbert space, and can thus be treated as an isolated system. This is the whole idea behind using the exchange coupling for the purpose of quantum gating. Moreover, as long as the Heisenberg Hamiltonian can be used to describe the quantum-dot two-spin system, the spin singlet and triplet states are always the exact eigenstates. The only important parameter for state evolution is the time integral of the Hamiltonian $\int H(\tau)d\tau$, and the exchange coupling should be turned on for as short a time as possible to produce an ultrafast gate. However, this time cannot be too short as to make the system ''leaky.'' Using the uncertainty principle, we can estimate the lower limit of this turn-on time τ_p. Recall that the next excited state of our two-electron system is about 8 meV above the ground states. Thus the lower limit of τ_p is about ($\delta E \sim 8$ meV is the energy difference between the next excited state and the ground singlet and triplet states)

$$\tau_p \gg \hbar / \delta E \sim 0.1 \text{ ps.} \qquad (17)$$

Therefore, as long as the gating time τ_p is longer than 1 ps in the current configuration, the coupled-dot system is well isolated, so that the higher excited states can be safely neglected, and the gating action can be considered adiabatic. This is critical for QC operation. Again a compromise is needed here to optimize a fast gating time and adiabaticity. Calculations of the kind carried out in our paper can provide quantitative estimates for such required QDQC architectural optimization.

According to Fig. 6, the exchange coupling J depends quite sensitively on the magnetic field **B**. If a sequential pulse algorithm is used, one does not need to worry about the interplay between the exchange interaction and the local magnetic field. On the other hand, if a parallel pulse scheme is used [48], one has to take into consideration the effect of the inhomogeneous magnetic field on the exchange coupling. Intuitively, the average field exchange coupling may be sufficient in many cases, because the single-electron wave-function radius decreases slowly as the magnetic field increases: $l_B = \sqrt{\hbar c / eB}$. If the average field is around zero, the field inhomogeneity may lead to a larger change in the exchange coupling, and will have to be taken into account.

Throughout our calculation we have neglected the Zeeman splitting of the electronic levels. This splitting cannot be ignored in a real unitary evolution. For instance, in Ref. [39] a pulse sequence was given for a controlled-NOT (CNOT) gate (the sequence as given is a conditional phase shift, which can be easily transformed into a CNOT operation). If a finite **B** field is present during the swap action, an additional phase due to Zeeman splitting of the triplet states will show up in the electron spin states. An opposite **B** field with the same strength has to be applied to the two electrons for the same amount of time as the swap gate to correct this phase error. For GaAs, the Zeeman splitting is about 0.03 meV/T. If a dot system has an exchange coupling of 0.1 meV and the two spins experience a magnetic field difference of 1 T, the corresponding difference in the Zeeman splitting would be 0.03 meV, about 30% of the exchange coupling, which is a significant number. Since an error rate below 10^{-4} is needed for the currently available error correction schemes to be effec-

tive, one has to be able to control the magnitude of the exchange interaction up to that accuracy. Furthermore, any residual local-field effect has to be corrected continuously. Indeed, if in an actual structure the gating area is separated from the storage area, which means that all the spins have to be transported to and from the gating area, one does not need to worry about the stray magnetic field. Here the main problem would be the transportation of the spins. On the other hand, if the spins are stored close to each other and the gating and storage areas are combined, the main problem would be the effects of the local stray magnetic field. It is straightforward to correct for the effect of a magnetic field on one spin. However, it is much less obvious how to correct for the effect of an inhomogeneous field on all but one spin in a chain. From an engineering perspective, the modular approach of separating storage and gating areas is somewhat more promising. We anticipate that the inhomogeneous field and the stray field problems to be significant obstacles in producing a successful QDQC architecture.

When electron transport is needed in an architecture, electron labeling becomes very important. In a semiconductor heterostructure, there always exist stray electrons, such as those trapped in impurities and deep levels. If we move our qubit electron around in a heterostructure, there is the danger of losing this electron, and in its place, acquiring a stray electron, so that all the spin information of the particular qubit is lost. The indistinguishable character of electrons becomes an important issue in this context. Initially, when all the electrons are trapped in their respective quantum dots, they are labeled and distinguishable. As soon as stray electrons are present outside the dot electrons we have considered, Pauli exchange errors will occur from the indistinguishability of fermions and have to be corrected [49]. This will be another significant obstacle for the QDQC architecture.

Experimentally, it is easier to deal with multiple electrons (instead of a single electron) in a quantum dot produced by modulating electric fields. Here it is hoped that certain shell structures exist (as we show in our results), so that such a quantum dot can be considered to be an effective spin-$\frac{1}{2}$ system. Multiple electrons may, however, make the indistinguishability problem a more prominent issue. However, one needs to keep in mind that the important question here is the spin state of the effective spin-$\frac{1}{2}$ system, not the spin state of any particular electron. We are currently pursuing multielectron calculations in order to better understand these difficult and complex issues.

If the exchange coupling J is tuned by changing external gate voltage in a QDQC, thermal fluctuations (or any other types of fluctuations) in the gate voltage will lead to fluctuations in J, thus causing phase errors in the swap gate that is crucial for two-qubit operations. Here we estimate this error by assuming a simple thermal (white) noise [17].

Assuming that $J=f(V)$, where J is the exchange coupling and V is the gate voltage that controls the value of J, around any particular value V_0, J can be expressed as $J(V)=J(V_0)+f'(V)|_{V_0}(V-V_0)$. During a swap gate between two quantum dots, the phase of the electronic spin wave function evolves as $\phi=\int_0^t J(\tau)d\tau/\hbar$. Thus the fluctuation in the phase ϕ is

$$\langle \delta\phi^2 \rangle = \langle \phi^2 \rangle - \langle \phi \rangle^2$$

$$= \frac{1}{\hbar^2}\int_0^t\int_0^t \langle \delta J(\tau_1)\delta J(\tau_2)\rangle d\tau_1 d\tau_2$$

$$\sim \int_0^t\int_0^t \frac{[f'(\bar V)]^2}{\hbar^2}\langle \delta V(\tau_1)\delta V(\tau_2)\rangle d\tau_1 d\tau_2.$$

$$(18)$$

If $|f'(\bar V)|$ is bounded by a constant α, we can replace it by α in the above expression. Furthermore, according to Nyquist theorem,

$$\langle \delta V(\tau_1)\delta V(\tau_2)\rangle = 4Rk_BT\delta(\tau_1-\tau_2). \quad (19)$$

Here R is the circuit resistance and T is the circuit temperature. We thus obtain the approximate expression for the phase fluctuation:

$$\langle \delta\phi^2 \rangle \sim 4Rk_BT\alpha^2t/\hbar^2. \quad (20)$$

In our calculation for double-quantum-dot QC architecture, V_b plays the role of external gate voltage. According to Fig. 9, in the two higher-barrier cases, J changes about 0.038 meV when V_b (the strength of the barrier Gaussian, not the effective barrier height) changes 1.83 meV. α can be obtained from this ratio as 0.021 eV/V. Assuming the swap gate is performed at 1 K (since J is in the order of 0.1 meV $\sim$ 1 K, the experimental temperature can only be lower than 1 K), and the transmission line connecting the gate to the outside has an impedance of 50 Ω, the rate for phase fluctuation $\langle \delta\phi^2 \rangle/t$ is about 3.2 MHz. The phase error accrued during a swap gate is about 0.06%. This is quite a small error which is of the same order of magnitude as the theoretical tolerance of the currently available quantum error correction codes. It should pose no problem to any demonstrative experiment. For a real quantum computer, this error rate needs to be further lowered by lowering experimental temperature and turning up J more gently (which requires longer time but produces smaller α) in the QDQC operation.

Indeed, the error discussed here, which originates from the interaction between the double dot and its external control, is relevant for all the other external ''knobs'' that are used to control the evolution of the double-dot states. To design a practical QDQC, one has to identify all the possible external noise sources and tunes the system parameters accordingly so as to prevent these noises from overwhelming the operations of the QDQC.

E. Future directions

In the current paper we studied in detail the Hilbert-space structure for a two-electron two-dot artificial hydrogen molecule situation. It is important to emphasize that detailed theoretical calculations of the type carried out in this paper will be critical in determining the feasibility and practicality of all the proposed semiconductor-based solid state QC architectures [14,16,17], not just the spin-based QDQC considered in our work. Given this crucial importance of theory in providing the QC architectural basis, it is quite surprising that no such detailed calculations have earlier been reported

in the literature in spite of very extensive research activity in the subject of QC. Indeed, there are many other theoretical questions that need to be answered for the quantum-dot quantum computer architecture. For example, an accurate description of the confinement potential is an important ingredient of a quantum computer, as quantum computation requires an exact knowledge of the qubit wave functions. In addition, currently there is no systematic calculation of spin relaxation in GaAs quantum dots, which will clearly be needed for a better understanding of spin coherence issues.

As for further improving the calculation of electron exchange coupling in the two-dot configuration, the main problem is to obtain a more accurate description of electron correlations. In the approaches we used in the current paper, the UHF method self-consistently evaluated single-particle wave functions, but only a single Slater determinant is used as the two-electron wave function. No two-electron correlation is included. On the other hand, the molecular-orbital method uses a small number of rigid single-electron wave functions (harmonic-well single-particle orbitals), but many two-electron orbitals are included to minimize the energy of the system. To improve upon the results obtained here, a self-consistent calculation with CI is needed. That is, one can solve the Hartree-Fock equations self-consistently, then use these HF wave functions as an improved basis to form a number of Slater determinants (instead of just one as in the HF calculation). The two-electron problem can then be solved on the basis of these Slater determinants. Generally, the larger the basis the more accurate is the result. Furthermore, a linear-combination-of-atomic-orbital approach can be used to partially solve the dilemma in the choice of gauge. Such CI calculations, which we are currently pursuing, are notoriously computationally demanding, and real progress toward truly realistic calculations is expected to be slow.

As it is very difficult to precisely trap a single electron in each quantum dot, one can consider using multielectron quantum dots as effective spin-$\frac{1}{2}$ qubits. Thus an important problem would be to study a multielectron two-dot system—in other words, a quantum dot Na_2 (or Cl_2, or others) molecule instead of H_2. The objective of such a calculation is twofold. First, at certain fillings there might exist effective spin-$\frac{1}{2}$ states for a multielectron system, so that the ''single-electron'' quantum-dot requirement in the current proposal can be relaxed. Second, such a calculation is also relevant in the general study of quantum dots. We are currently pursuing such calculations as well.

VI. CONCLUSION

We have studied a quantum-dot hydrogen molecule as the basic elementary gate for a quantum computer based on electron spins in quantum dots. By using both Hartree-Fock approximation and a molecular-orbital theory, we determine the excitation spectrum of two electrons in two horizontally coupled quantum dots, and study its dependence on an external magnetic field. We particularly focus on the splitting

of the lowest singlet and triplet states—the exchange coupling, the double occupation probability of the lowest states, and the relative energy scales of these states. We find that in our chosen configuration and for reasonable GaAs dot-based parameters the exchange coupling has a maximum of about 0.2–1.1 meV at zero magnetic field as we vary the central barrier height from about 9.61–3.38 meV when the dots are separated by 30 nm. When the interdot separation increases to 40 nm, the exchange coupling decreases to below 0.3 meV. There exists a singlet-triplet crossing for all the cases for an applied magnetic field of about 4 T, above which the triplet state becomes the ground state of the two-electron system. At zero magnetic field, the double occupation probability in the ground singlet state is found to be as large as 22% with a 3.38-meV central barrier when the two dots are separated by 30 nm, and as small as 1.7% with a 11.03-meV central barrier when the interdot distance is 40 nm. Both the exchange coupling and the double occupation probability have similar dependence on the interdot distance and the central barrier height at zero magnetic field, so that it is difficult to have a configuration with large exchange coupling and vanishing double occupation probability (which means a vanishingly small error rate). At finite magnetic field, on the other hand, it is possible to have a finite (albeit negative) exchange coupling and a small double occupation probability simultaneously. We discuss in detail the necessary conditions for the validity of the effective-mass envelope-function approach, finding this approximation to be valid for our problem. We also discuss the applicability of various quantum-chemical approaches in the current context of quantum-dot quantum computation in dealing with few-electron problems, such as the Hartree-Fock self-consistent-field method, the molecular-orbital method, the Heisenberg model, and the Hubbard model. In particular, we point out that a configuration-interaction calculation is needed for any realistic description of electron wave functions. The difference between the non-product form of a Slater determinant and a truly entangled state is discussed. The presence of singlet-triplet crossing in a coupled-dot system is also studied. In addition, we discuss various important issues in quantum-dot quantum computing, such as controls needed, spin decoherence channels in semiconductors, adiabatic transitions, and errors in spin evolution. Our results should form a reasonable semirealistic basis for discussing spin-based quantum-dot quantum computer architectures, and should also be useful for various studies of quantum dot artificial molecule systems.

[1] D. P. DiVincenzo, Science **270**, 255 (1995); A. Ekert and R. Jozsa, Rev. Mod. Phys. **68**, 733 (1996); A. Steane, Rep. Prog. Phys. **61**, 117 (1998).

[2] P. W. Shor, in *Proceedings of the 35th Annual Symposium on the Foundations of Computer Science*, edited by S. Goldwasser (IEEE Computer Society, Los Alamitos, CA, 1994), p. 124.

[3] L. K. Grover, Phys. Rev. Lett. **79**, 325 (1997).

[4] R. P. Feynman, Int. J. Theor. Phys. **21**, 467 (1982); Found. Phys. **16**, 507 (1986).

[5] S. Somaroo, C. H. Tseng, T. F. Havel, R. Laflamme, and D. G. Cory, Phys. Rev. Lett. **82**, 5381 (1999).

[6] P. W. Shor, Phys. Rev. A **52**, 2493 (1995); A. M. Steane, Phys. Rev. Lett. **77**, 793 (1996).

[7] D. P. DiVincenzo, in *Mesoscopic Electron Transport*, edited by L. L. Sohn, L. P. Kouwenhoven, and G. Schön (Kluwer, Dordrecht, 1997).

[8] J. I. Cirac and P. Zoller, Phys. Rev. Lett. **74**, 4091 (1995).

[9] C. Monroe, D. M. Meekhof, B. E. King, W. M. Itano, and D. J. Wineland, Phys. Rev. Lett. **75**, 4714 (1995).

[10] T. Sleator and H. Weinfurter, Phys. Rev. Lett. **74**, 4087 (1995).

[11] Q. A. Turchette, C. J. Hood, W. Lange, H. Marbuchi, and H. J. Kimble, Phys. Rev. Lett. **75**, 4710 (1995).

[12] D. G. Cory, A. F. Fahmy, and T. F. Havel, Proc. Natl. Acad. Sci. USA **94**, 1634 (1997); N. A. Gershenfeld and I. L. Chuang, Science **275**, 350 (1997).

[13] A. Shnirman, G. Schön, and Z. Hermon, Phys. Rev. Lett. **79**, 2371 (1997); D. V. Averin, Solid State Commun. **105**, 659 (1998).

[14] D. Loss and D. P. DiVincenzo, Phys. Rev. A **57**, 120 (1998).

[15] A. Imamoglu, D. D. Awschalom, G. Burkard, D. P. DiVincenzo, D. Loss, M. Sherwin, and A. Small, Phys. Rev. Lett. **83**, 4204 (1999).

[16] N. H. Bonadeo, J. Erland, D. Gammon, D. Park, D. S. Katzer, and D. G. Steel, Science **282**, 1473 (1998).

[17] B. E. Kane, Nature (London) **393**, 133 (1998); V. Privman, I. D. Vagner, and G. Kventsel, Phys. Lett. A **239**, 141 (1998).

[18] J. Fabian and S. Das Sarma, Phys. Rev. Lett. **81**, 5624 (1998); **83**, 1211 (1999); J. Appl. Phys. **85**, 5075 (1999).

[19] J. Fabian and S. Das Sarma, J. Vac. Sci. Technol. B **17**, 1708 (1999).

[20] B. E. Kane, N. S. McAlpine, A. S. Dzurak, R. G. Clark, G. J. Milburn, H. B. Sun, and H. Wiseman, LANL e-print cond-mat/9903371.

[21] L. Jacak, P. Hawrylak, and A. Wójs, *Quantum Dots* (Springer, Berlin, 1997).

[22] R. C. Ashoori, Nature (London) **379**, 413 (1996).

[23] U. Merkt, J. Huser, and M. Wagner, Phys. Rev. B **43**, 7320 (1991).

[24] D. Pfannkuche, V. Gudmundsson, and P. A. Maksym, Phys. Rev. B **47**, 2244 (1993).

[25] J. J. Palacios and P. Hawrylak, Phys. Rev. B **51**, 1769 (1995).

[26] H. Tamura, Physica B **249-251**, 210 (1998).

[27] Y. Asano, Phys. Rev. B **58**, 1414 (1998).

[28] B. Partoens, A. Matulis, and F. M. Peeters, Phys. Rev. B **59**, 1617 (1999).

[29] G. Burkard, G. Seelig, and D. Loss, LANL e-print cond-mat/9910105.

[30] T. Schmidt, R. J. Haug, K. v. Klitzing, A. Föster, and H. Lüth, Phys. Rev. Lett. **78**, 1544 (1997).

[31] D. G. Austing, T. Honda, K. Muraki, Y. Tokura, and S. Tarucha, Physica B **249-251**, 206 (1998).

[32] T. H. Oosterkamp, T. Fujisawa, W. G. van der Wiel, K. Ishibashi, R. V. Hijman, S. Tarucha, and L. P. Kouwenhoven, Nature (London) **395**, 873 (1998).

[33] T. Fujisawa, T. H. Oosterkamp, W. G. van der Wiel, B. W. Broer, R. Aguado, S. Tarucha, and L. P. Kouwenhoven, Science **282**, 932 (1998).

[34] F. R. Waugh, M. J. Berry, D. J. Mar, R. M. Westervelt, K. L. Campman, and A. C. Gossard, Phys. Rev. Lett. **75**, 705 (1995).

[35] C. Livermore, C. H. Crouch, R. M. Westervelt, K. L. Campman, and A. C. Gossard, Science **274**, 1332 (1996); R. Kotlyar and S. Das Sarma, Phys. Rev. B **56**, 13 235 (1997).

[36] T. H. Oosterkamp, S. F. Godijn, M. J. Uilenreef, Y. V. Nazarov, N. C. van der Vaart, and L. P. Kouwenhoven, Phys. Rev. Lett. **80**, 4951 (1998).

[37] R. H. Blick, D. Pfannkuche, R. J. Haug, K. v Klitzing, and K. Eberl, Phys. Rev. Lett. **80**, 4032 (1998); R. H. Blick, D. W. van der Weide, R. J. Haug, and K. Eberl, *ibid.* **81**, 689 (1998).

[38] C. Yannouleas and U. Landman, Phys. Rev. Lett. **82**, 5325 (1999).

[39] G. Burkard, D. Loss, and D. P. DiVincenzo, Phys. Rev. B **59**, 2070 (1999).

[40] J. C. Slater, *Quantum Theory of Molecules and Solids* (McGraw-Hill, New York, 1963), Vol. 1; R. McWeeny, *Methods of Molecular Quantum Mechanics* (Academic Press, San Diego, 1992).

[41] N. W. Ashcroft and N. D. Mermin, *Solid State Physics* (Saunders, New York, 1976).

[42] G. Bastard, *Wave Mechanics Applied to Semiconductor Heterostructures* (Halsted, New York, 1988).

[43] M. Wagner, U. Merkt, and A. V. Chaplik, Phys. Rev. B **45**, 1951 (1992).

[44] C. Herring, in *Magnetism*, edited by G. T. Rado and H. Suhl (Academic Press, New York, 1966), Vol. 4.

[45] A. Auerbach, *Interacting Electrons and Quantum Magnetism* (Springer-Verlag, New York, 1994).

[46] C. A. Stafford and S. Das Sarma, Phys. Rev. Lett. **72**, 3590 (1994); R. Kotlyar, C. A. Stafford, and S. Das Sarma, Phys. Rev. B **58**, 3989 (1998).

[47] J. M. Kikkawa and D. D. Awschalom, Nature (London) **397**, 139 (1999); Phys. Rev. Lett. **80**, 4313 (1998); J. M. Kikkawa *et al.*, Science **277**, 1284 (1997).

[48] G. Burkard, D. Loss, D. P. DiVincenzo, and J. A. Smolin, Phys. Rev. B **60**, 114 04 (1999).

[49] M. B. Ruskai, LANL e-print quant-ph/9906114.